

PAUL SCHERRER INSTITUT



Aeroradiometric Measurements in the Framework of the Swiss Exercises ARM14 and FTX14

Gernot Butterweck, Benno Bucher, Ladislaus Rybach, Georg Schwarz,
Eike Hohmann, Sabine Mayer, Cristina Danzi, Gerald Scharding

PSI Bericht Nr. 15-02

May 2015

ISSN 1019-0643

Aeroradiometric Measurements in the Framework of the Swiss Exercises ARM14 and FTX14

Gernot Butterweck¹, Benno Bucher², Ladislaus Rybach³, Georg Schwarz²,
Eike Hohmann¹, Sabine Mayer¹, Cristina Danzi⁴, Gerald Scharding⁴

- 1 Division for Radiation Safety and Security, Paul Scherrer Institute (PSI),
5232 Villigen PSI, Switzerland
- 2 Swiss Federal Nuclear Safety Inspectorate (ENSI), Industriestrasse 19,
5200 Brugg, Switzerland
- 3 Institute of Geophysics, Swiss Federal Institute of Technology Zürich (ETHZ),
8092 Zürich, Switzerland
- 4 Swiss National Emergency Operations Center (NEOC),
8044 Zürich, Switzerland

Paul Scherrer Institut (PSI)
5232 Villigen PSI, Switzerland
Tel. +41 56 310 21 11
Fax +41 56 310 21 99
www.psi.ch

PSI Bericht Nr. 15-02
May 2015
ISSN 1019-0643



ABSTRACT

The measurement flights of the exercise ARM14 were performed between June 2nd and 6th, 2014. The exercise was organized by the National Emergency Operations Centre (NEOC) under coordination from the Expert Group for Aeroradiometrics (FAR). According to the alternating schedule of the annual ARM exercises, the environs of the nuclear power plants Beznau (KKB) and Leibstadt (KKL) and the nuclear facilities of the Paul Scherrer Institute (PSI) and the Zwischenlager Würenlingen AG (Zwilag) were surveyed. Following a request of the German authorities, the measuring area was extended beyond the Rhine River into German territory. As in previous years, the distinction between pressurized and boiling water reactor is clearly identified.

The series of radiological background measurements over Swiss cities was complemented with measurements over Brugg, Baden, Schaffhausen and Winterthur.

A new detector was characterised in the laboratory and tested successfully during the exercise. Test with the prototype of a new airborne gamma spectrometry system showed deficiencies in the proprietary software for data evaluation, which will be mended by the manufacturer. The raw measuring data rendered comparable results to the existing system when evaluated with the existing data evaluation software.

Several source search exercises during ARM14, its sub-exercise RadEx14 and the international military exercise FTX14 yielded valuable information on the performance of the airborne gamma spectrometry system and its limitations.

CONTENTS

1	INTRODUCTION	1
1.1	Measuring System	1
1.2	Characterisation of spectroscopic performance	2
1.3	Measuring flights	4
1.4	Data evaluation	5
1.5	Data presentation	5
2	RESULTS OF THE MEASURING FLIGHTS	7
2.1	Recurrent measurement area KKL, KKB, PSI and Zwilag including Baden and Brugg.....	8
2.2	Schaffhausen	13
2.3	Winterthur.....	17
2.4	Intercomparison of detectors.....	20
2.5	Exercise RadEx14.....	25
2.6	Exercise FTX14.....	27
2.7	Profile St. Gallen - Maloja	37
2.8	Profile Koppigen - Zurich.....	40
3	CONCLUSIONS	42
4	LITERATURE	43
5	PREVIOUS REPORTS	43
6	EVALUATION PARAMETER FILES.....	45
6.1	DefinitionFile_Processing.txt.....	45
6.2	Processing_Quellensuche.txt.....	47
6.3	DefinitionFile_DetA.txt.....	49
6.4	DefinitionFile_DetC.txt	52
6.5	DefinitionFile_DetD.txt	54

TABLES

Table 1: Ratio of counts in the energy windows	3
Table 2: Quantification of the color scale	6
Table 3: Flight data of ARM14.....	7
Table 4: Average activity concentrations over the Thorium anomaly at Rotbergegg	23
Table 5: Source activities in the intercomparison area	25
Table 6: Radioactive sources in the exercise area and measured activities.	28

FIGURES

Figure 1: Measurement system of the Swiss team.....	2
Figure 2: Super Puma Helicopter of the Swiss Air Force.	2
Figure 3: Spectrum of ^{232}Th and energy windows for the evaluation.....	3
Figure 4: Detector D mounted in the calibration laboratory	4
Figure 5: Dose rate in the vicinity of KKL, KKB, PSI and ZWILAG including Baden and Brugg.	9
Figure 6: MMGC-ratio in the vicinity of KKL, KKB, PSI and ZWILAG including Baden and Brugg.	10
Figure 7: ^{232}Th activity concentration in the vicinity of KKL, KKB, PSI and ZWILAG including Baden and Brugg.....	11
Figure 8: ^{40}K activity concentration in the vicinity of KKL, KKB, PSI and ZWILAG including Baden and Brugg.....	12
Figure 9: Dose rate in the vicinity of Schaffhausen.	13
Figure 10: MMGC-ratio in the vicinity of Schaffhausen.	14
Figure 11: ^{232}Th activity concentration in the vicinity of Schaffhausen.	15
Figure 12: ^{40}K activity concentration in the vicinity of Schaffhausen.	16
Figure 13: Dose rate in the vicinity of Winterthur.....	17
Figure 14: Terrestrial component of the dose rate in the vicinity of Winterthur.....	18
Figure 15: MMGC-ratio in the vicinity of Winterthur.....	19
Figure 16: ^{232}Th activity concentration in the vicinity of Winterthur.....	20
Figure 17: Comparison of raw spectra averaged over the measuring area.....	21
Figure 18: Arial view of the intercomparison area. Source positions are marked with crosses (green - ^{137}Cs , red - ^{60}Co).	22
Figure 19: ^{232}Th activity concentration measured with detector D in the intercomparison area.....	23
Figure 20: MMGC-ratio in the intercomparison area determined with detector RLL.	24
Figure 21: Photon spectra measured over the OAHC building with three detectors. 25	
Figure 22: Flight lines and location of the exercise area near Frauenfeld.	26
Figure 23: MMGC-ratio in the exercise area. Source positions are marked with green crosses.	27
Figure 24: Positions of the radioactive sources in the exercise area (crosses; green - ^{137}Cs , red - ^{60}Co , blue - ^{133}Ba , black - ^{241}Am).	28
Figure 25: MMGC-ratio in the exercise area.	29

Figure 26: Terrestrial component of the dose rate in the exercise area.	30
Figure 27: Photon spectrum measured near the ^{241}Am -source.	31
Figure 28: Photon spectrum averaged over the indicated area around coordinate (515426, 152888).	32
Figure 29: Estimated ^{137}Cs -point-source activity in the exercise area.	33
Figure 30: Photon spectrum averaged over the indicated area around coordinate (514055, 153909).	34
Figure 31: Rescaled MMGC-ratio in the exercise area.	35
Figure 32: Photon spectrum averaged over the indicated area around coordinate (515289, 153239).	36
Figure 33: Photon spectrum averaged over the indicated area around coordinate (515071, 153398).	36
Figure 34: Estimated ^{60}Co -point-source activity in the exercise area.	37
Figure 35: Flight line of the profile from St. Gallen to Maloja.	38
Figure 36: Terrestrial dose rate along the profile from St. Gallen to Maloja.	39
Figure 37: ^{232}Th activity concentration along the profile from St. Gallen to Maloja. ...	39
Figure 38: Flight line of the profile from Koppigen to Zurich.	40
Figure 39: Terrestrial dose rate along the profile from Koppigen to Zurich.	41
Figure 40: Height above ground along the profile from Koppigen to Zurich.	41

1 INTRODUCTION

Swiss airborne gamma spectrometry measurements started in 1986. Methodology and software for calibration, data acquisition and mapping were developed at the Institute of Geophysics of the Swiss Federal Institute of Technology Zurich (ETHZ). Between 1989 and 1993 the environs of Swiss nuclear installations were measured annually on behalf of the Swiss Federal Nuclear Safety Inspectorate (ENSI). This schedule was changed to biannual inspections in 1994, together with an organizational inclusion of the airborne gamma-spectrometric system into the Emergency Organization Radioactivity (EOR) of the Federal Office for Civil Protection (FOCP). The deployment of the airborne gamma-spectrometric system is organized by the National Emergency Operations Centre (NEOC). NEOC is also responsible for the recruitment and instruction of the measurement team. Aerial operations are coordinated and performed by the Swiss Air Force. The gamma-spectrometric equipment is stationed at the military airfield of Dübendorf. The gamma-spectrometry system can be airborne within four hours. Responsibility for scientific support, development and maintenance of the aeroradiometric measurement equipment passed from ETHZ to the Radiation Metrology Section of the Paul Scherrer Institute (PSI) in 2003 in cooperation with ENSI. General scientific coordination and planning of the annual measuring flights is provided by the Expert Group for Aeroradiometrics (FAR). FAR was a working group of the Swiss Federal Commission for NBC-protection (ComNBC) and consists of experts from all Swiss institutions concerned with aeroradiometry. FAR was re-organized as an expert group of the NEOC in 2008. Additional information can be found at <http://www.far.ensi.ch/>.

This report focusses on methodological aspects and thus complements the short report of NEOC about the annual flight surveys (available from the NEOC website <https://www.naz.ch>).

1.1 Measuring System

The measuring system consists of four NaI-detectors with a total volume of 16.8 l. The measurements of ARM14 were performed with a new detector package (Detector D, Radiation Solutions RSX4) which includes digital spectrometers with a maximum resolution of 1024 channels for each detector, which replaced the separate spectrometer of the electronics rack. To render the data evaluation compatible to the old systems, the spectral resolution is reduced to 256 channels. The measurement control, data acquisition and storage are performed with an industrial grade personal computer. A second, identically configured PC is present in the electronics rack (Figure 1) as redundancy. Under normal operation conditions, this PC is used for real-time evaluation and mapping of the data. The positioning uses GPS (Global Positioning System) in the improved EGNOS (European Geostationary Navigation Overlay Service) mode. Together with spectrum and position, air pressure, air temperature and radar altitude are registered. The measuring system is mounted in an Aérospatiale AS 332 Super Puma helicopter of the Swiss Air Force (Figure 2). This helicopter has excellent navigation properties and allows emergency operation during bad weather conditions and nighttime. The detector is mounted in the cargo bay

below the center of the helicopter. The cargo bay is covered with a lightweight honeycomb plate to minimize photon absorption losses.

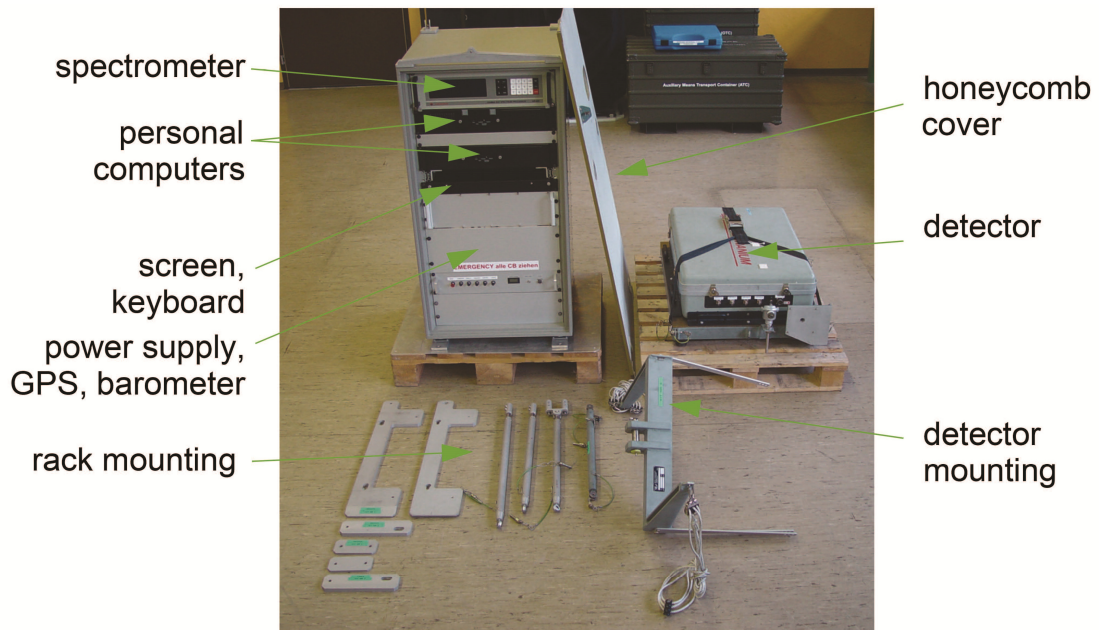


Figure 1: Measurement system of the Swiss team.



Figure 2: Super Puma Helicopter of the Swiss Air Force.

1.2 Characterisation of spectroscopic performance

The evaluation of the spectra uses energy windows to determine activities or activity concentrations of different radionuclides. Due to emission characteristics, Compton-Scattering and the energy resolution of the detectors, photons originating from a specific radionuclide may be registered in energy windows assigned for a different radio-

nuclide. For illustration, Figure 3 shows the spectrum of a ^{232}Th -source including the background of the irradiation room (black curve) and the different energy windows used for the spectrum evaluation (vertical lines).

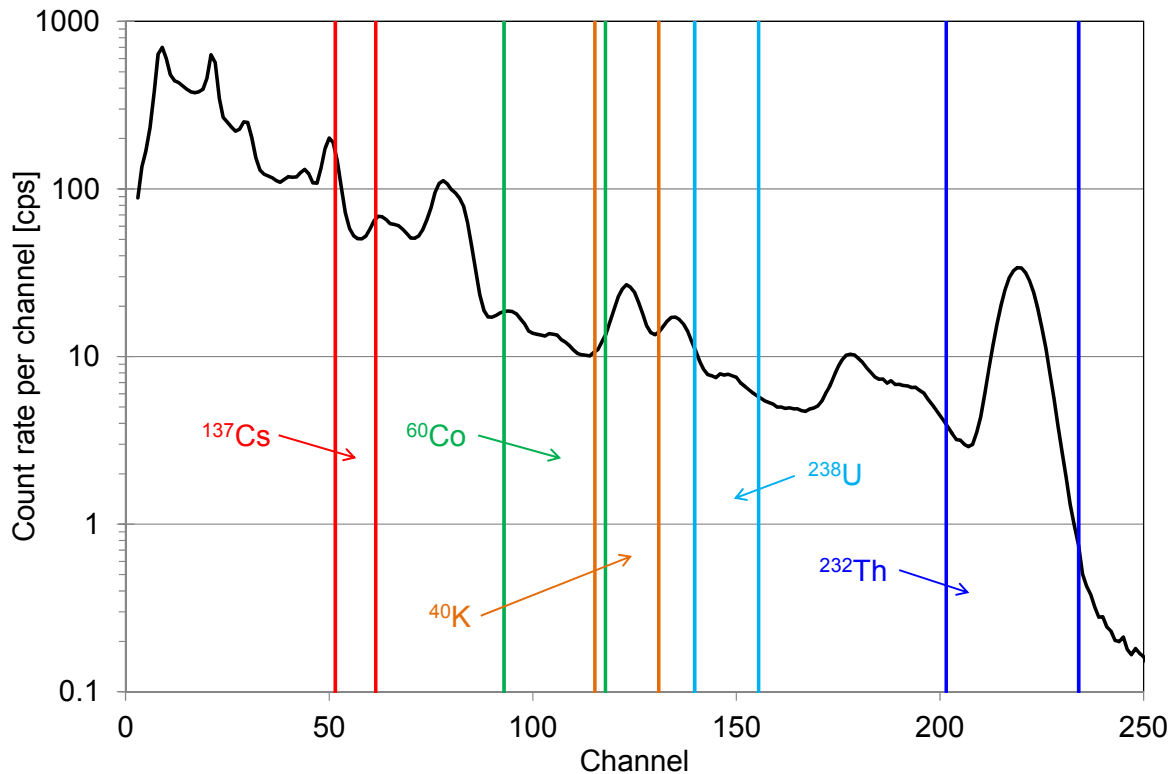


Figure 3: Spectrum of ^{232}Th and energy windows for the evaluation

The influence of a given radionuclide to a specific energy window has to be determined experimentally for the quantification of correction factors of the measured count rates (stripping correction matrix). The ratio of the measured counts from each source in each energy window to the counts in the energy windows assigned to the radionuclide (Table 1) are the basis for the stripping correction matrix stored in the detector definition file (see section 6).

Table 1: Ratio of counts in the energy windows

		Radionuclide				
		Potassium	Uranium	Thorium	Caesium	Cobalt
Energy Window	Potassium	1.0	0.8	0.3	0.0	0.1
	Uranium	0.0	1.0	0.2	0.0	0.0
	Thorium	0.0	0.1	1.0	0.0	0.0
	Caesium	0.1	3.0	1.4	1.0	0.2
	Cobalt	0.3	2.2	0.5	0.0	1.0

These measurements were performed at the calibration laboratory for radiation protection instruments of the Paul Scherrer Institute (PSI). Quantitative measurements were performed in the reference radiation fields of the calibration laboratory. The estimation of spectral performance was measured with radionuclide sources of various geometries which is considered sufficient for the determination of the relative response in different energy windows. Figure 4 shows the new detector D mounted for the measurement of the spectrum of a ^{40}K -source. The new digital spectrometer of detector D mounted directly in the detector box renders measurements up to a dose rate of $4 \mu\text{Sv/h}$ at the location of the detector possible, which is about a factor of 10 larger than the maximum permitted dose of the old spectrometers used with detectors A and C.

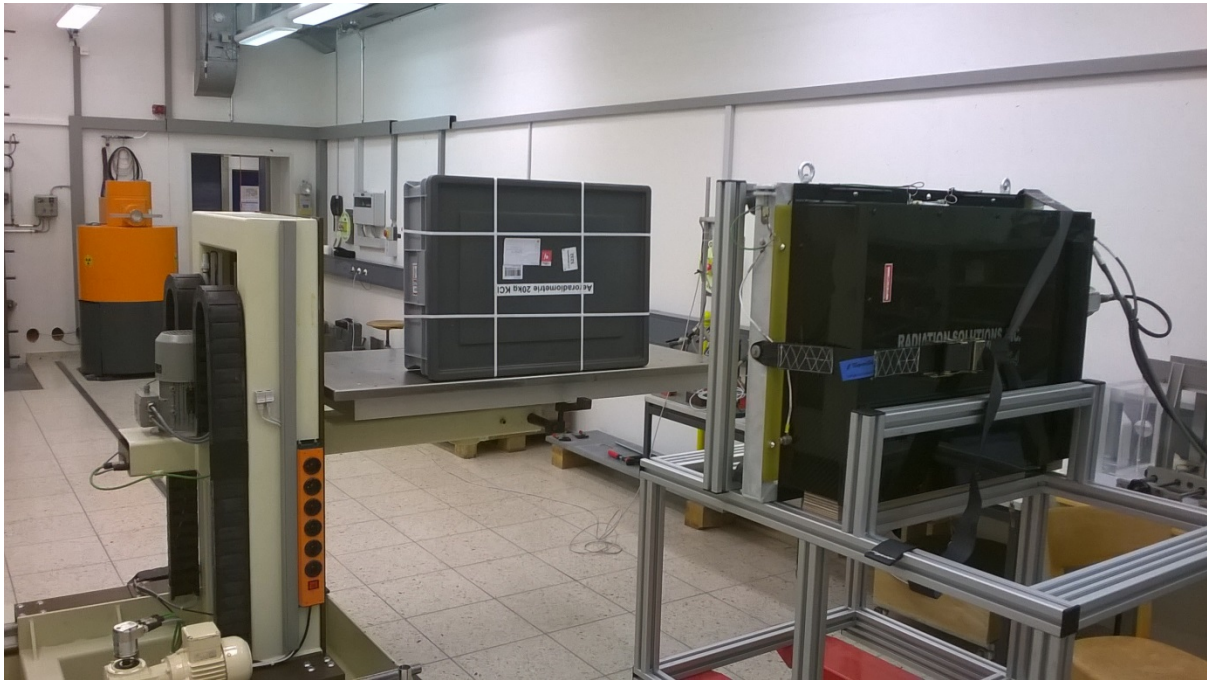


Figure 4: Detector D mounted in the calibration laboratory

Triggered by the determination of the stripping correction matrix of the new detector D, the according matrices of the old detectors A and C based on measurements performed in 2007 were re-evaluated using now consistently quadratic energy calibrations. The respective detector definition files named according to the detector identifier DefinitionFile_DetA.txt, DefinitionFile_DetC.txt and DefinitionFile_DetD.txt were revised accordingly (see section 6).

1.3 Measuring flights

The advantage of aeroradiometric measurements lies in the high velocity of measurements in a large area, even over rough terrain. Uniform radiological information of an area is obtained from a regular grid of measuring points. This grid is composed from parallel flight lines which are 100 m to 500 m apart, depending on the scope of the measurement. The flight altitude above ground is aspired to be constant during the measuring flight. Typical values lie between 50 m and 100 m above ground. The

spectra are recorded in regular time intervals of typical one second, yielding integration over 28 meters of the flight line at a velocity of 100 km/h.

1.4 Data evaluation

The data evaluation follows the methodology described in Schwarz (1991). Since the year 2000, software developed by the Research Group for Geothermics and Radiometry of the Institute of Geophysics of the Swiss Federal Institute of Technology Zurich (ETHZ) with on-line mapping options (Bucher, 2001) is used. Starting with this report, the revised definition files as stated in section 6 were used for the data evaluation.

1.5 Data presentation

A first brief report (Kurzbericht) of the measurement results is compiled by the measurement team and published immediately after the end of the exercise on the homepage of NEOC. These reports are archived at <http://www.far.ensi.ch>.

Results of a further data evaluation are published in the form of a PSI-report. For all measuring areas, a map of the total dose rate (measuring quantity $H^*(10)$ at 1 m above ground) and the flight lines is presented together with a map of the Man-Made-Gross-Count (MMGC) ratio.






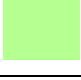





A map of the ^{232}Th activity concentration (measuring quantity activity per dry mass) yields quality information as it can be expected that this quantity is constant over time. As an additional quality measure, an appendix with the basic parameters of the data evaluation is added to simplify a re-evaluation of the data in the future.

If the MMGC-ratio indicates elevated values, maps of individual radionuclides are added based on the average photon spectrum over the affected area.

In the case of large changes of topography in the measured area, a map of the terrestrial dose rate consisting of the total dose rate reduced of the altitude dependent cosmic component is included. In the case of measuring flights with the main purpose of mapping natural radionuclide concentrations, a supplementary map of the ^{40}K activity concentration (measuring quantity activity per wet mass) is presented.

All maps use a gradual color scale from blue for low values to red for high values. The maximum and minimum values are specified in the legend together with the measurement unit of the depicted quantity. The colors for 10 percent steps between minimum and maximum values of the scale are given in Table 2.

Table 2: Quantification of the color scale

Percentage	Color
≥ 100	
90	
80	
70	
60	
50	
40	
30	
20	
10	
≤ 0	

2 RESULTS OF THE MEASURING FLIGHTS DURING THE EXERCISE ARM14

The flights of the exercise ARM14 were performed with a Super Puma helicopter of the Swiss Air Force between June 2nd and 6th, 2014. Personnel of the military unit Stab BR NAZ performed the measurements supported by experts from ENSI, PSI and NEOC. Representatives of KomZenABC-Kamir participated in the comparison measurements between different detectors at PSI, see Chapter 2.4. A short report with preliminary measurement results was placed on the NEOC website <https://www.naz.ch/> on June 6th, 2014. The results presented in the short report were evaluated using the old detector definition file of detector A and a provisional detector definition file for detector D based on the old detector definition file of detector C. Nevertheless, the results of the short report agree within the measurement uncertainties with the results presented in this report.

Flight parameters of ARM14 are listed in Table 3. Flight velocity of all measuring flights was around 30 m/s with a ground clearance of 90 m. The counting interval of the spectra was one second.

Table 3: Flight data of ARM14

Location	Flight number	Date	Effective measuring time [s]	Length of run [km]	Area [km ²]
KKL, KKB, PSI, ZWILAG, Brugg and Baden	2014103	2.6.2014	19931	1056	600
	2014105				
	2014106				
	2014117	3.6.2014			
	2014118				
	2014119	4.6.2014			
	2014120				
	2014128				
Schaffhausen	2014122	3.6.2014	2061	90	23
Winterthur	2014123	3.6.2014	3710	170	41
Intercomparison	2014202	6.6.2014	5619	215	26
	2014137				
RadEx14	2014132	5.6.2014	201	7	0.1
FTX14	1995002	17.11.2014	2734	81	1.7
	2095001				
St. Gallen - Maloja	2014126	4.6.2014	4752	208	-
Koppigen - Zurich	2001001	17.11.2014	1073	74	-

2.1 Recurrent measurement area KKL, KKB, PSI and Zwilag including Baden and Brugg

According to a biannual rotation of routine measurements, the environs of the nuclear power plants Leibstadt (KKL) and Beznau (KKB), the Paul Scherrer Institute (PSI) and the intermediate storage facility (ZWILAG) were inspected in 2014. Following a request from German authorities, the measuring area was extended to the north into German territory. An area to the south was added to the routine measurement area including the cities of Brugg and Baden to extend the knowledge on the radiological background of Switzerland.

The dose rate map (Figure 5) shows elevated values over KKL, Rotbergegg and in the north-west of the measuring area, whereas KKB, PSI and ZWILAG are unobtrusive. With the exception of the plant premises of KKL, no indication of artificial radionuclides visible in higher values of the MMGC-ratio (Figure 6) was detected. The elevated dose rate over the premises of KKL is caused by high energy photon radiation of the activation product ^{16}N , a typical result for operating boiling water reactors. The high energy photon radiation of ^{16}N leads to misinterpretations in the maps of ^{232}Th (Figure 7) and ^{40}K (Figure 8). The elevated dose rate at Rotbergegg is due to a known anomaly of the natural radionuclide ^{232}Th , which can be clearly seen in the ^{232}Th map (Figure 7). The slightly increased dose rate in the north-west of the measuring area can be attributed to increased concentrations of the natural radionuclide ^{40}K (Figure 8).

Parts of the area were measured with a 250 m spacing of the flight lines, whereas for the area to the south a spacing of 1000 m was used. From the spectra along the flight lines, values are interpolated to a grid raster for mapping. The optimal cell size for this process is half the line spacing. Thus, the areas measured with different line spacing were projected to two different grids with cell sizes of 125 m and 500 m, respectively. The grids are plotted slightly transparent to show the underlying topographical map. Due to the superposition in overlapping parts of the grids this transparency is reduced. This is clearly observable in the maps of the MMGC-ratio (Figure 6) and the ^{40}K activity concentration (Figure 8).

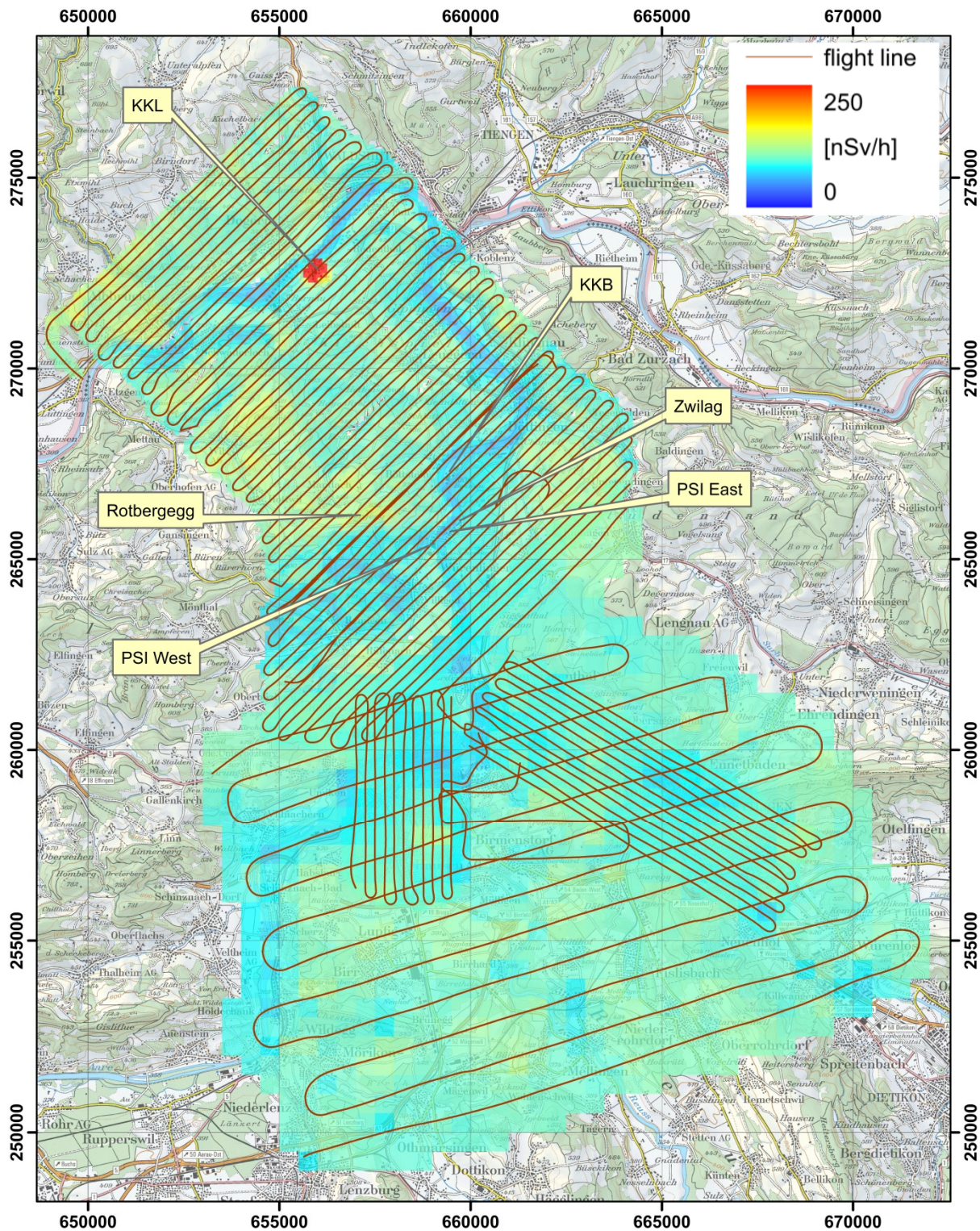


Figure 5: Dose rate in the vicinity of KKL, KKB, PSI and ZWILAG including Baden and Brugg. PK100 © 2015 swisstopo (JD100042)

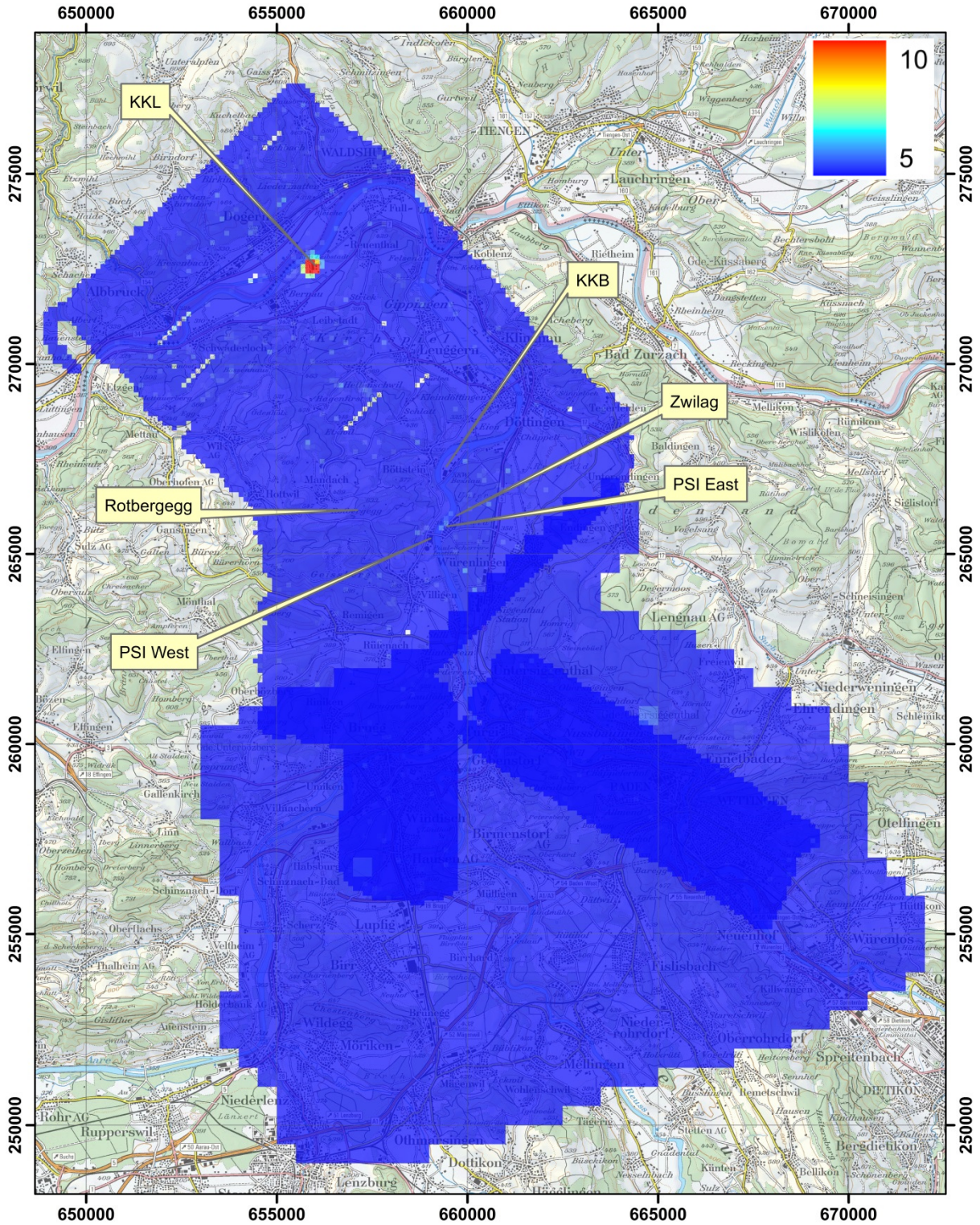


Figure 6: MMGC-ratio in the vicinity of KKL, KKB, PSI and ZWILAG including Baden and Brugg. PK100 © 2015 swisstopo (JD100042)

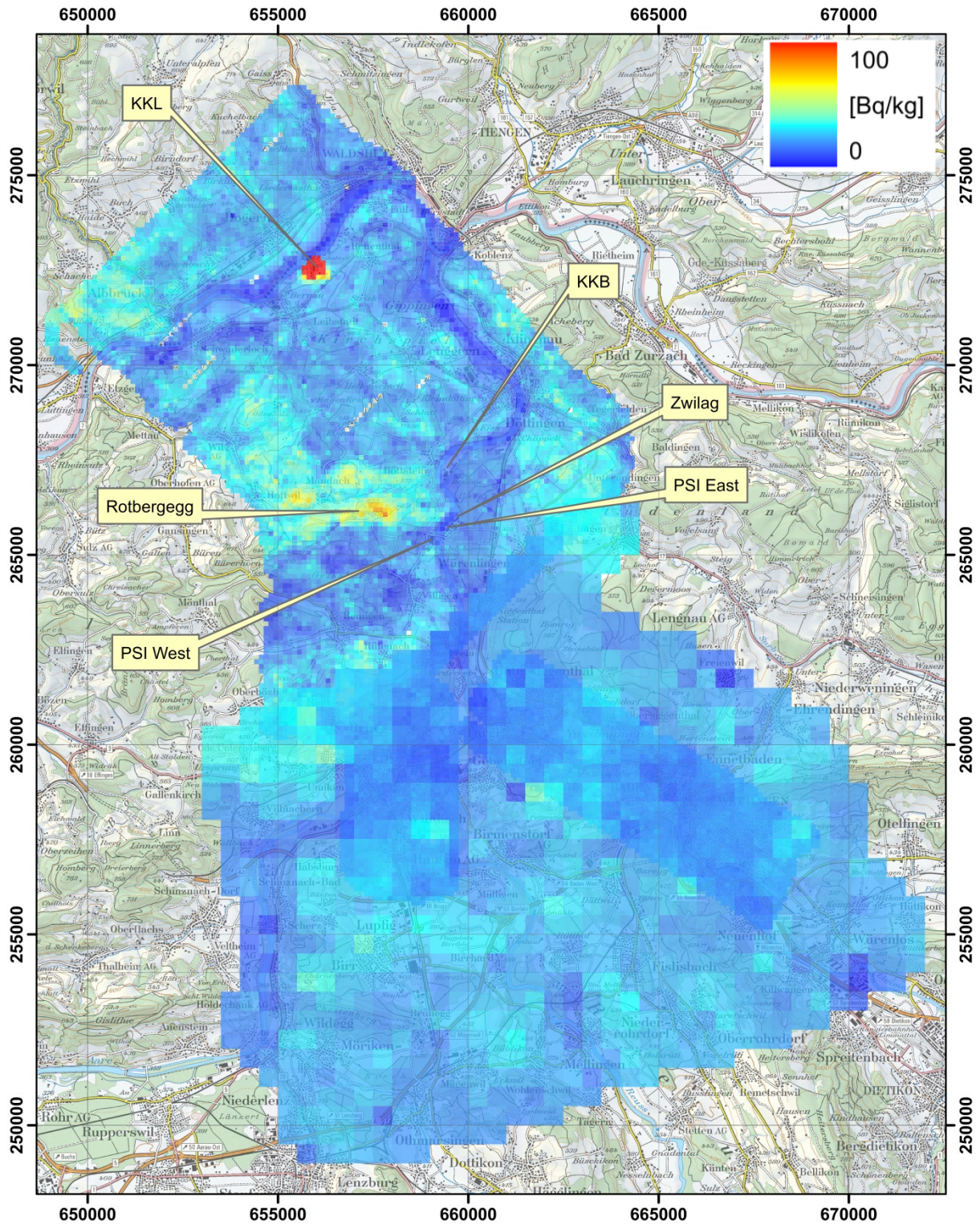


Figure 7: ^{232}Th activity concentration in the vicinity of KKL, KKB, PSI and ZWILAG including Baden and Brugg. PK100 © 2015 swisstopo (JD10042)

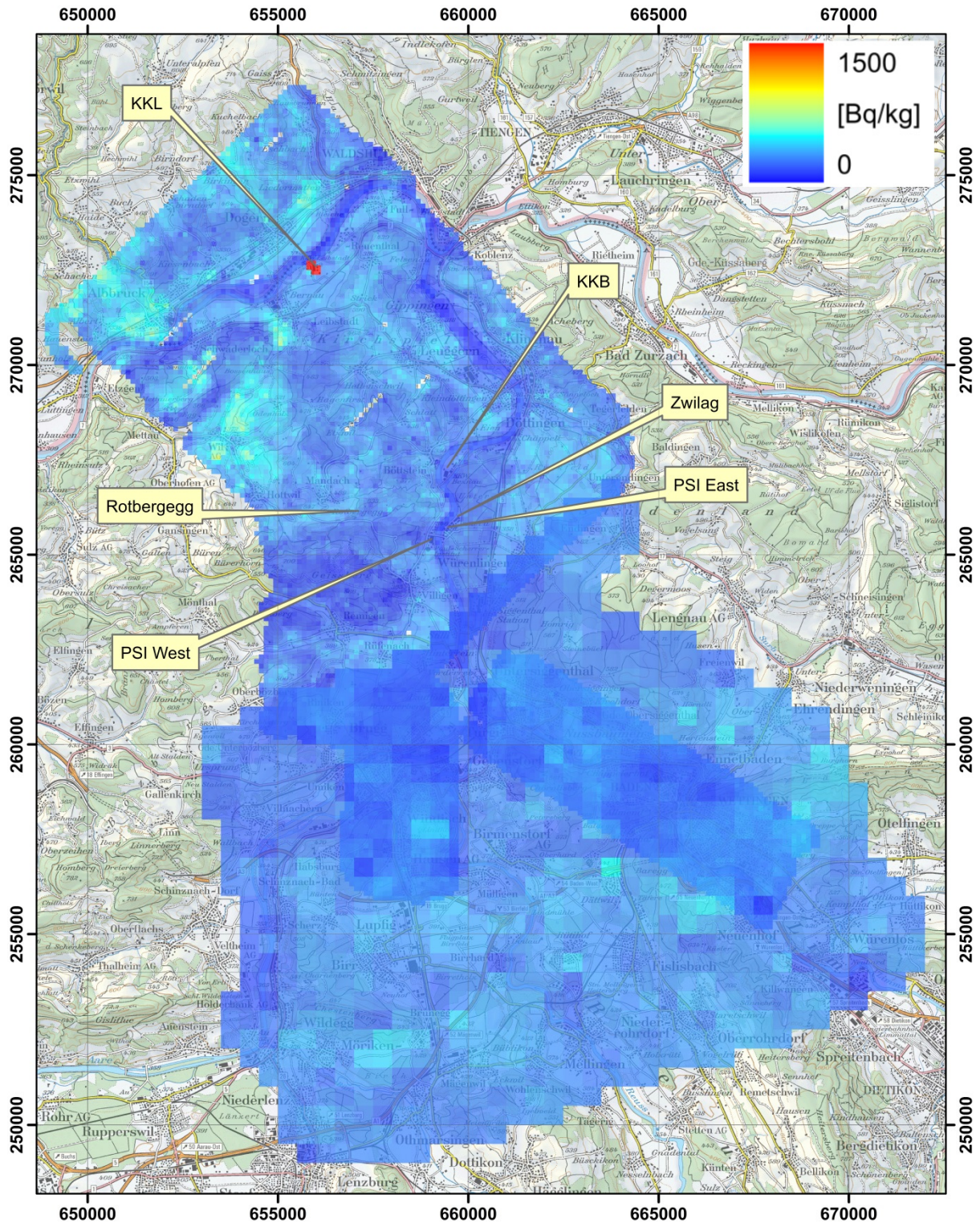


Figure 8: ^{40}K activity concentration in the vicinity of KKL, KKB, PSI and ZWILAG including Baden and Brugg. PK100 © 2015 swisstopo (JD100042)

2.2 Schaffhausen

For the extension of the series of radiological background maps over Swiss cities, the vicinity of Schaffhausen was measured during ARM14. A slight increase of dose rate can be observed south-east of the Rhine Falls located at coordinate (688395, 281475) (Figure 9). The map of the MMGC-ratio (Figure 10) yields no indication of artificial radionuclides in the complete measured area. The dose rate increase can be attributed to elevated concentrations of natural radionuclides, especially ^{40}K (Figure 11 and Figure 12).

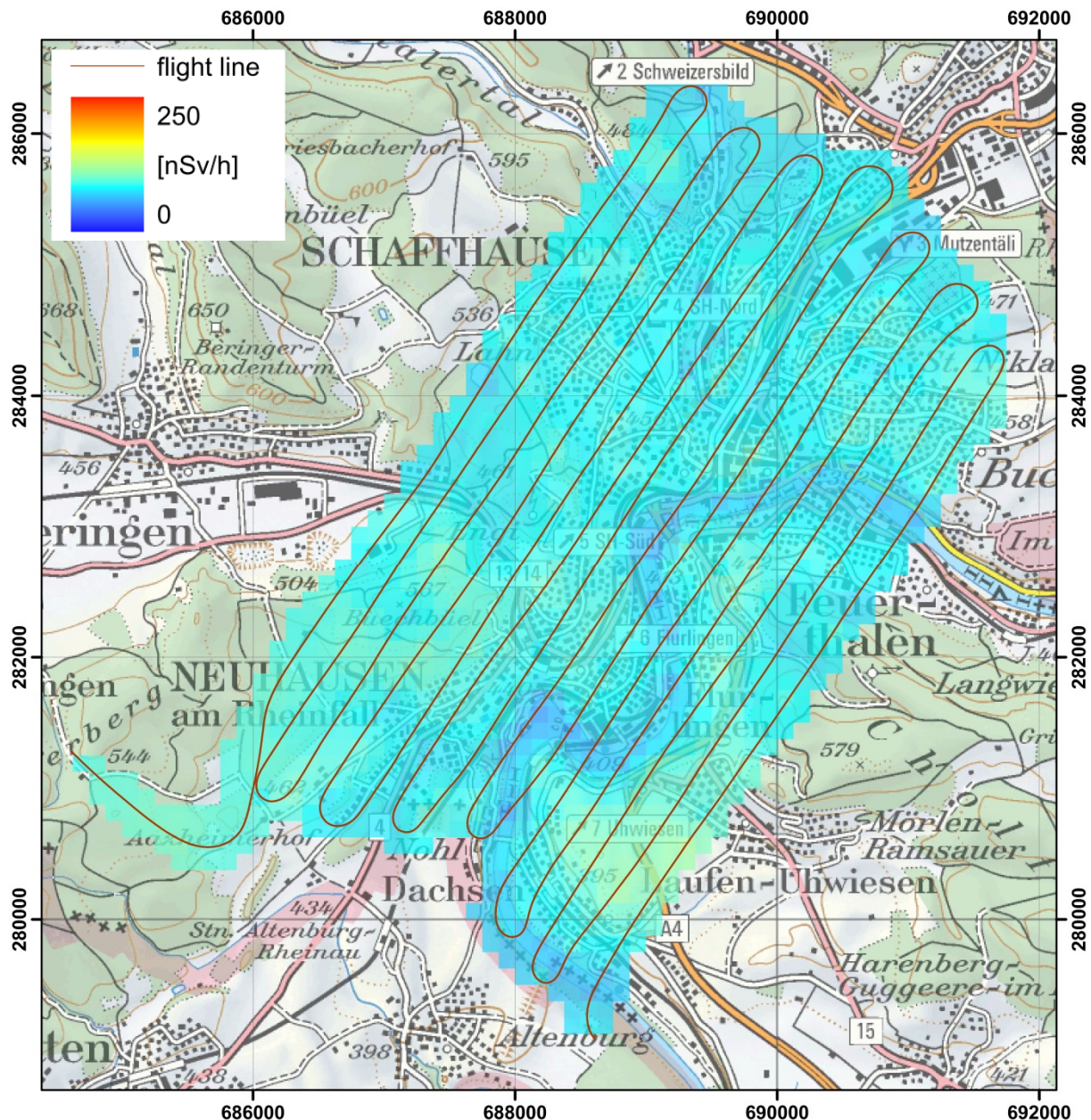


Figure 9: Dose rate in the vicinity of Schaffhausen. PK100 © 2015 swisstopo (JD100042)

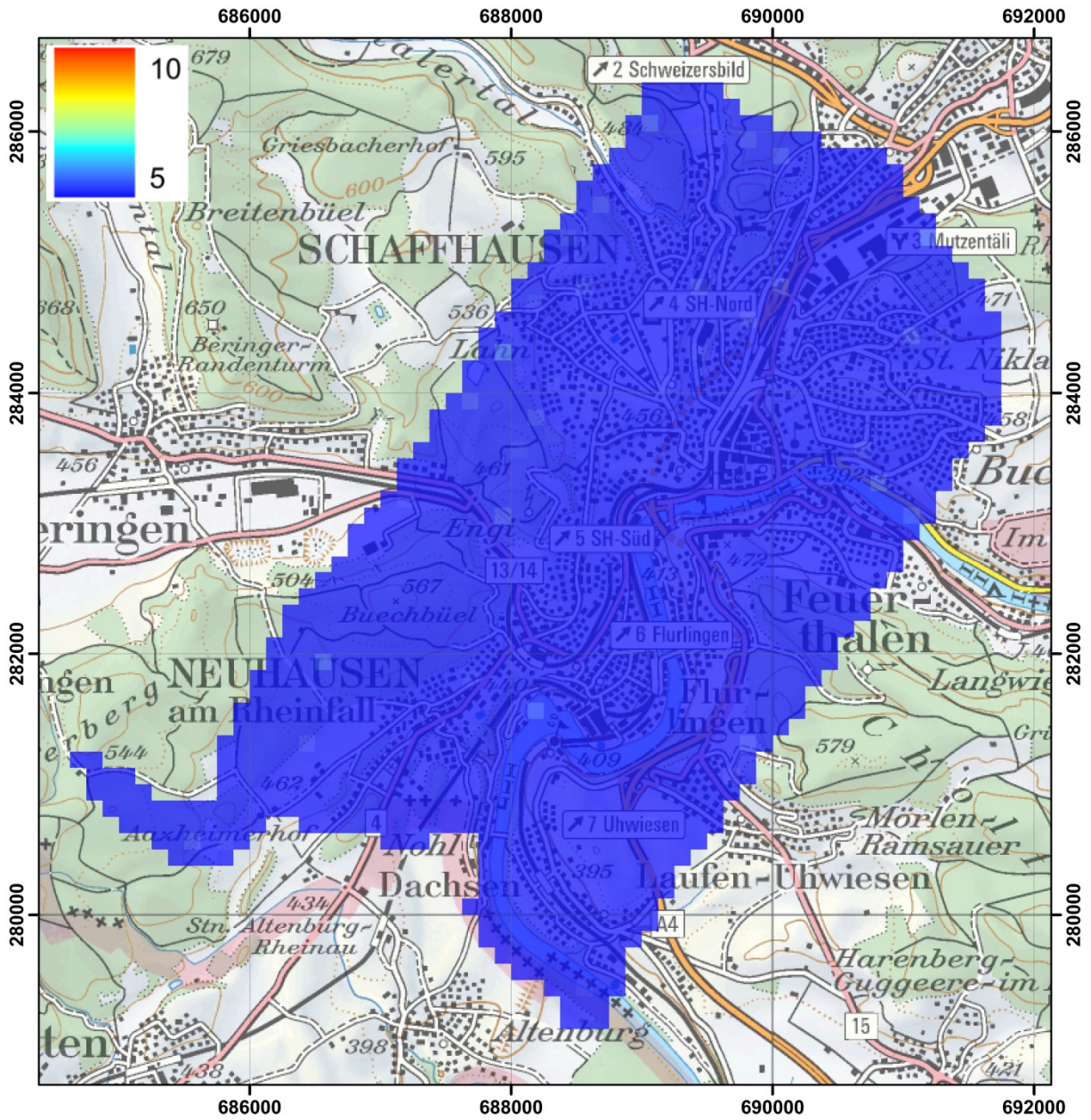


Figure 10: MMGC-ratio in the vicinity of Schaffhausen. PK100 © 2015 swisstopo (JD100042)

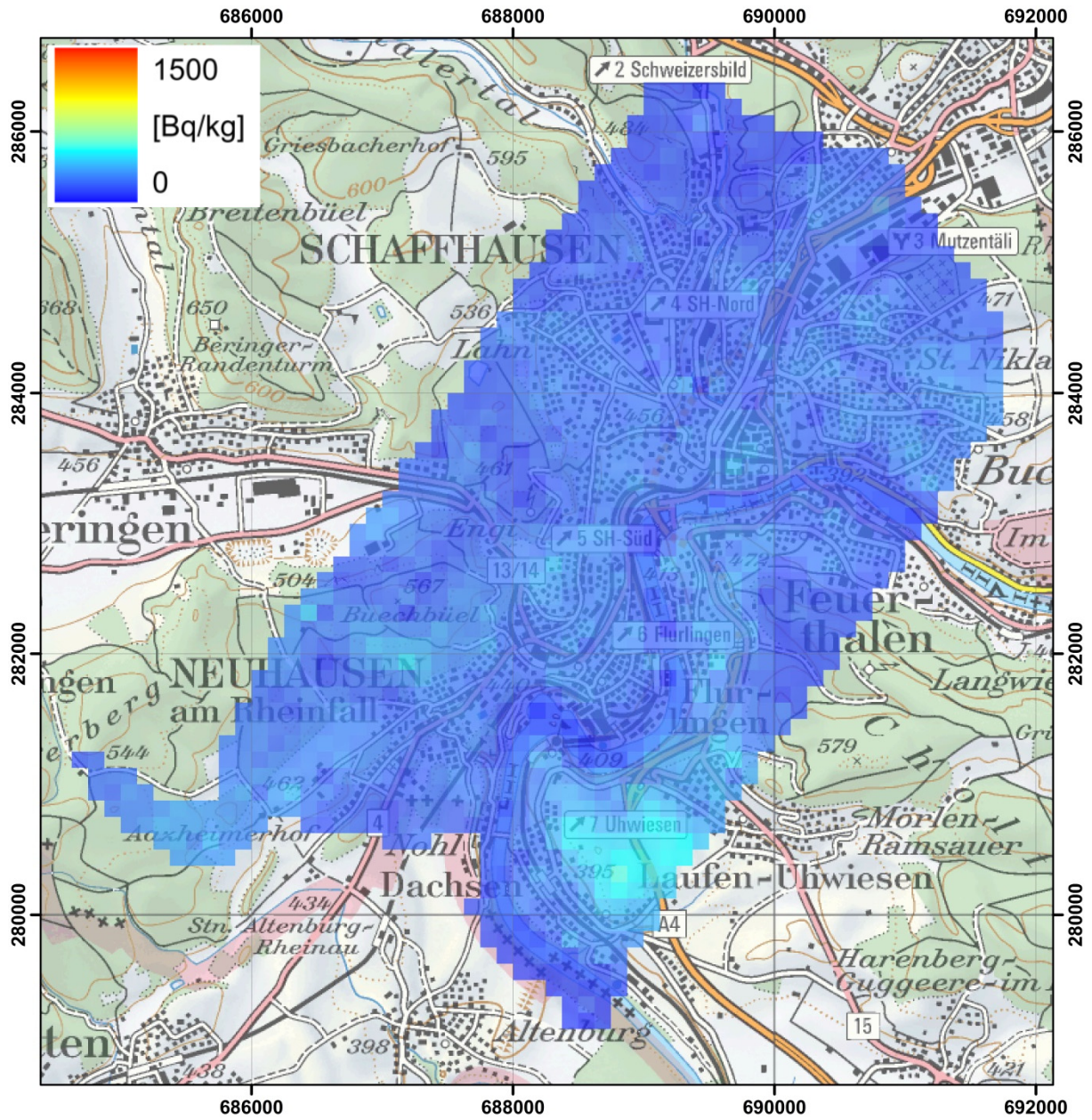


Figure 12: ^{40}K activity concentration in the vicinity of Schaffhausen. PK100 © 2015 swisstopo (JD100042)

2.3 Winterthur

For the extension of the series of radiological background maps over Swiss cities, the vicinity of Winterthur was measured during ARM14. Spatial fluctuations in the dose rate (Figure 13) are associated with the terrain of the measured area. The terrestrial component of the dose rate (Figure 14), which does not include the altitude dependent cosmic component shows a more uniform distribution. The map of the MMGC-ratio (Figure 15) gives no indication of artificial radionuclides in the measured area. The map of the ^{232}Th activity concentration (Figure 16), presented mainly as an indication of data quality, depicts no noticeable features.

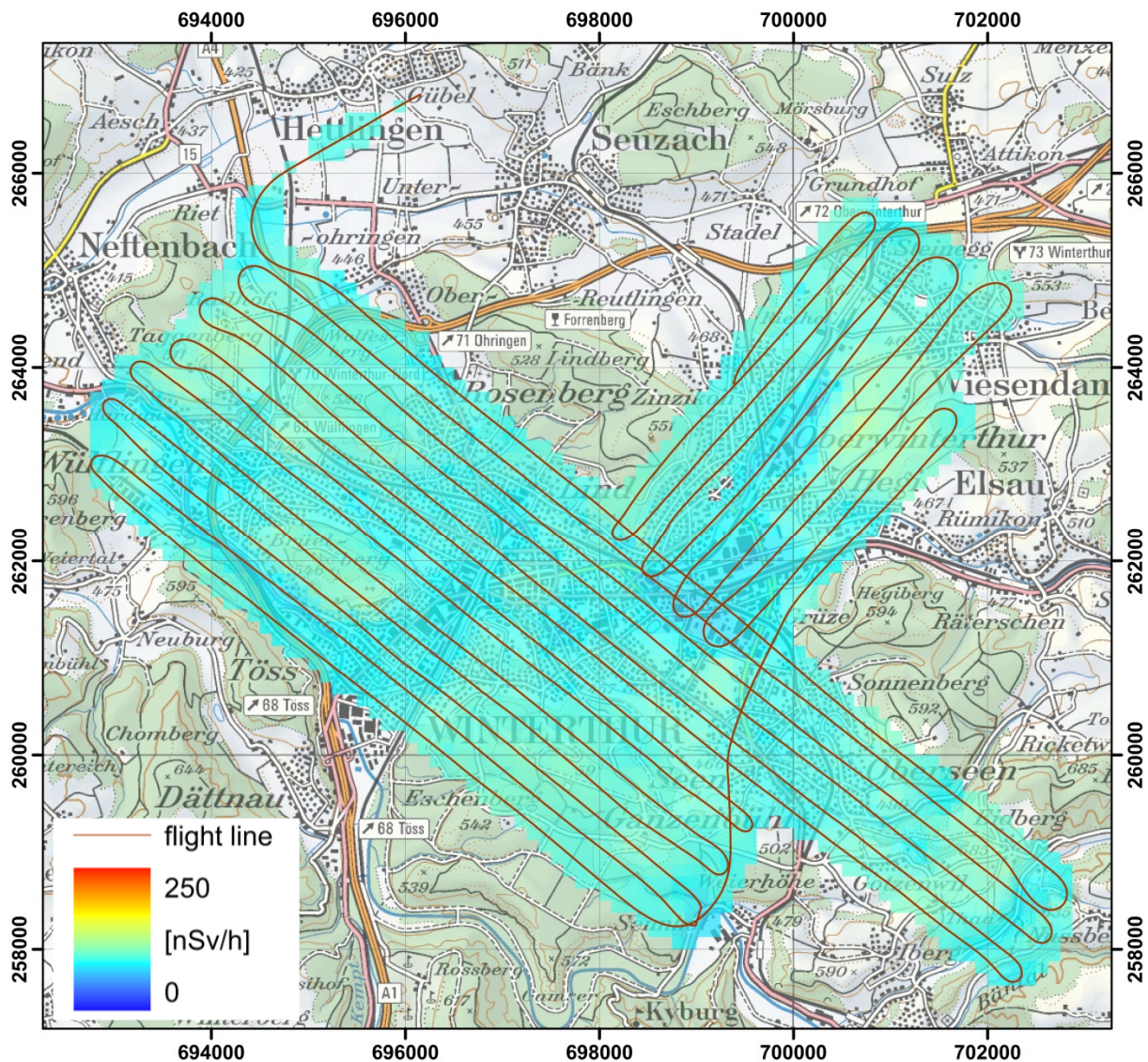


Figure 13: Dose rate in the vicinity of Winterthur. PK100 © 2015 swisstopo (JD100042)

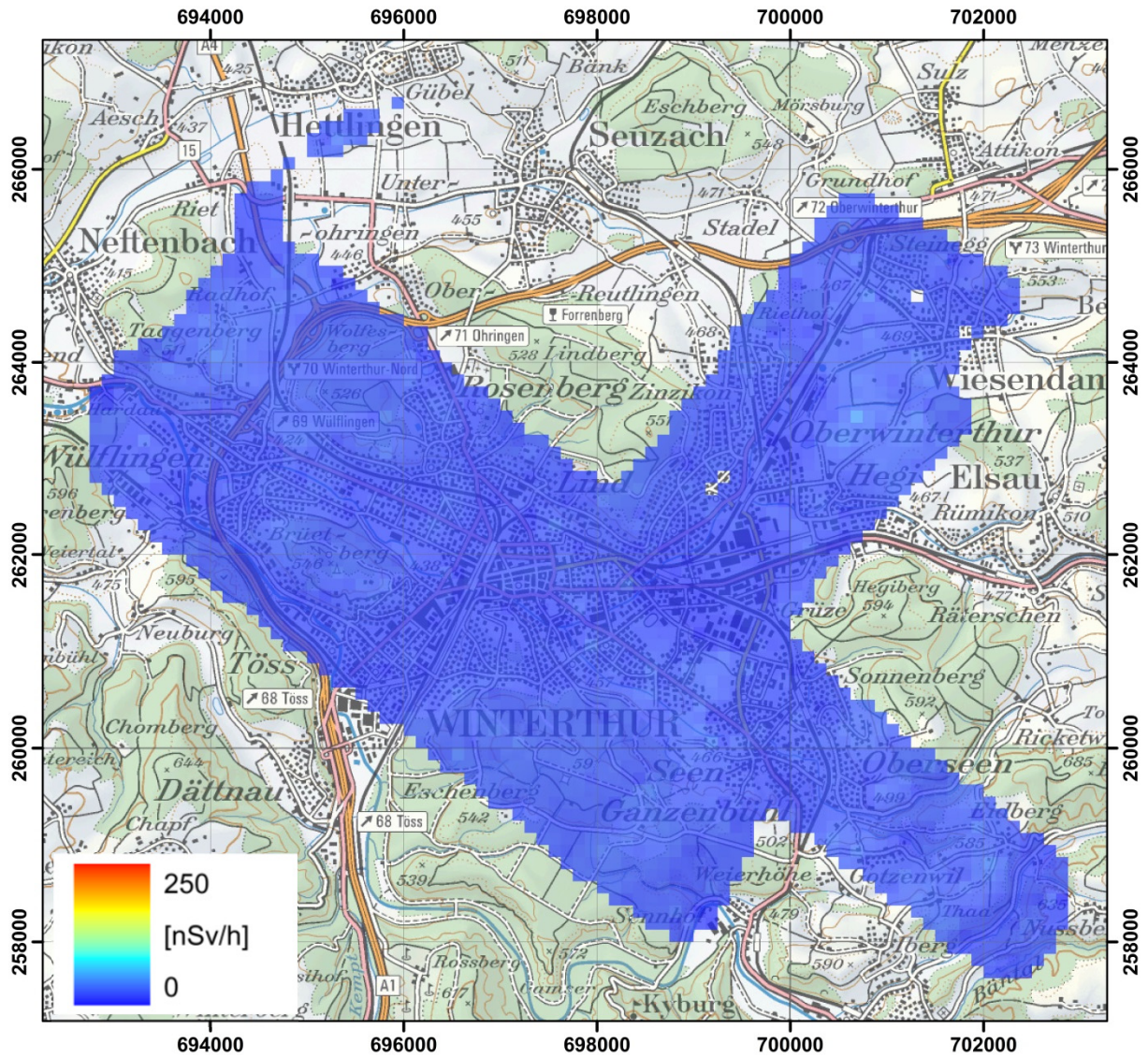


Figure 14: Terrestrial component of the dose rate in the vicinity of Winterthur.
PK100 © 2015 swisstopo (JD100042)

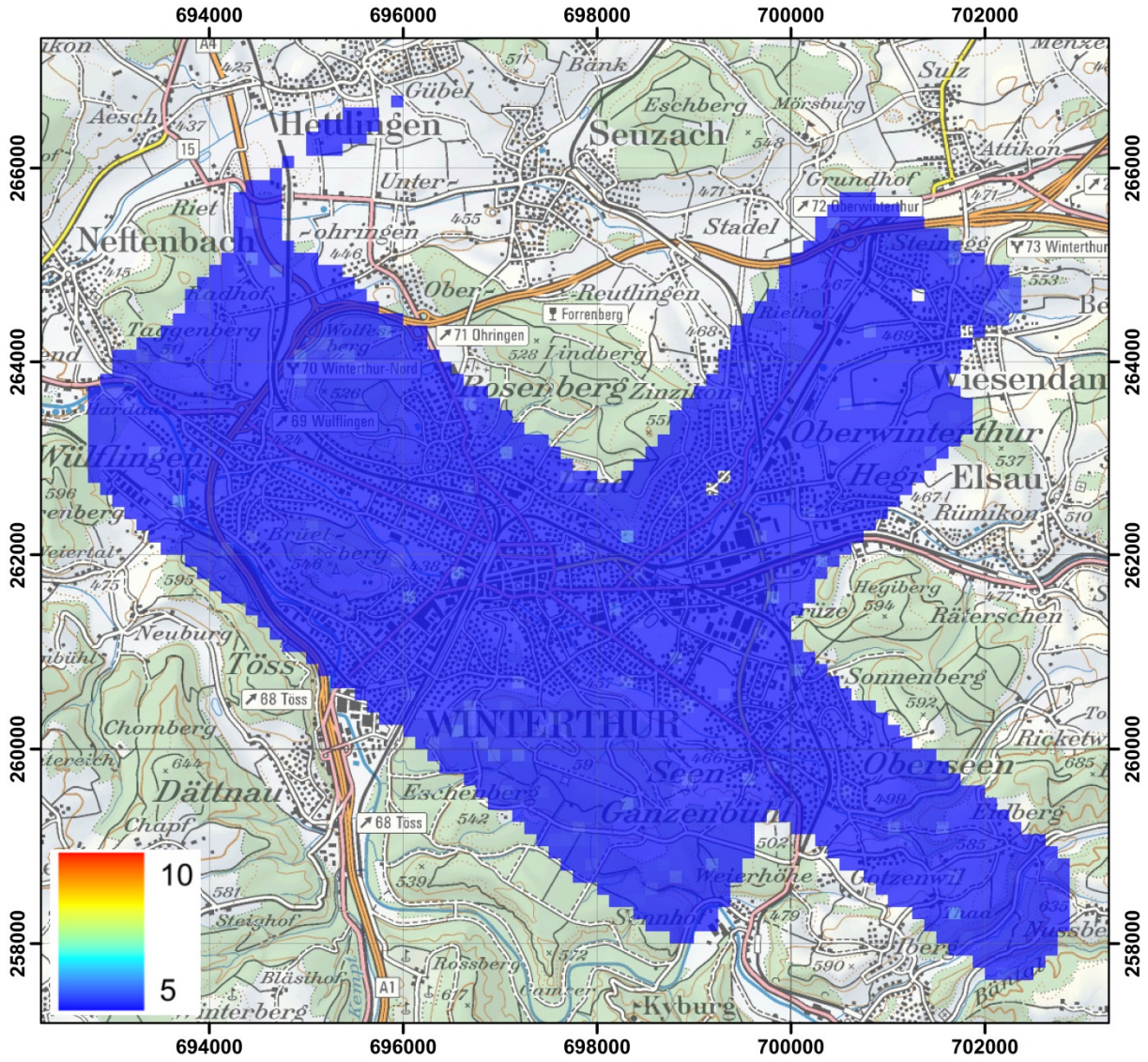


Figure 15: MMGC-ratio in the vicinity of Winterthur. PK100 © 2015 swisstopo (JD100042)

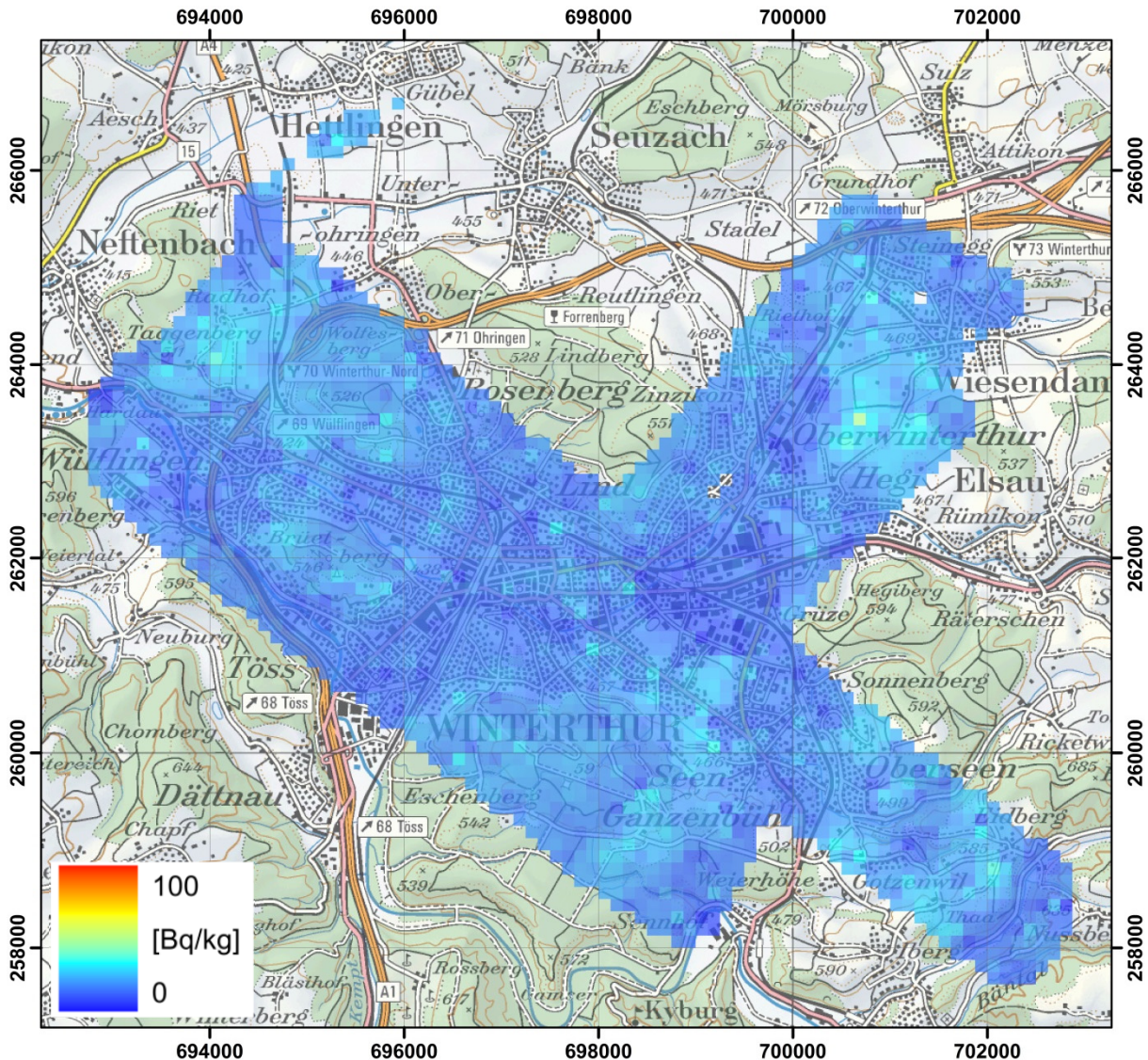


Figure 16: ^{232}Th activity concentration in the vicinity of Winterthur. PK100 © 2015 swisstopo (JD100042)

2.4 Intercomparison of detectors

A prototype of a new airborne gamma spectrometry system (detector RLL) was tested during ARM14 over the environs of the Paul Scherrer Institute (PSI). The results were compared to parallel measurements with two existing detectors (detector A and detector D). Unfortunately, the results showed that the proprietary data evaluation software provided by the manufacturer of the prototype did not achieve the design targets, especially concerning the calibration of the system. Therefore, the RLL raw data were evaluated using the existing data evaluation software, assuming, that the characteristics of the RLL-detector were identical to those determined for detector D. This assumption is based on the nearly identical average raw spectra of detector D and detector RLL over the complete measurement area (Figure 17).

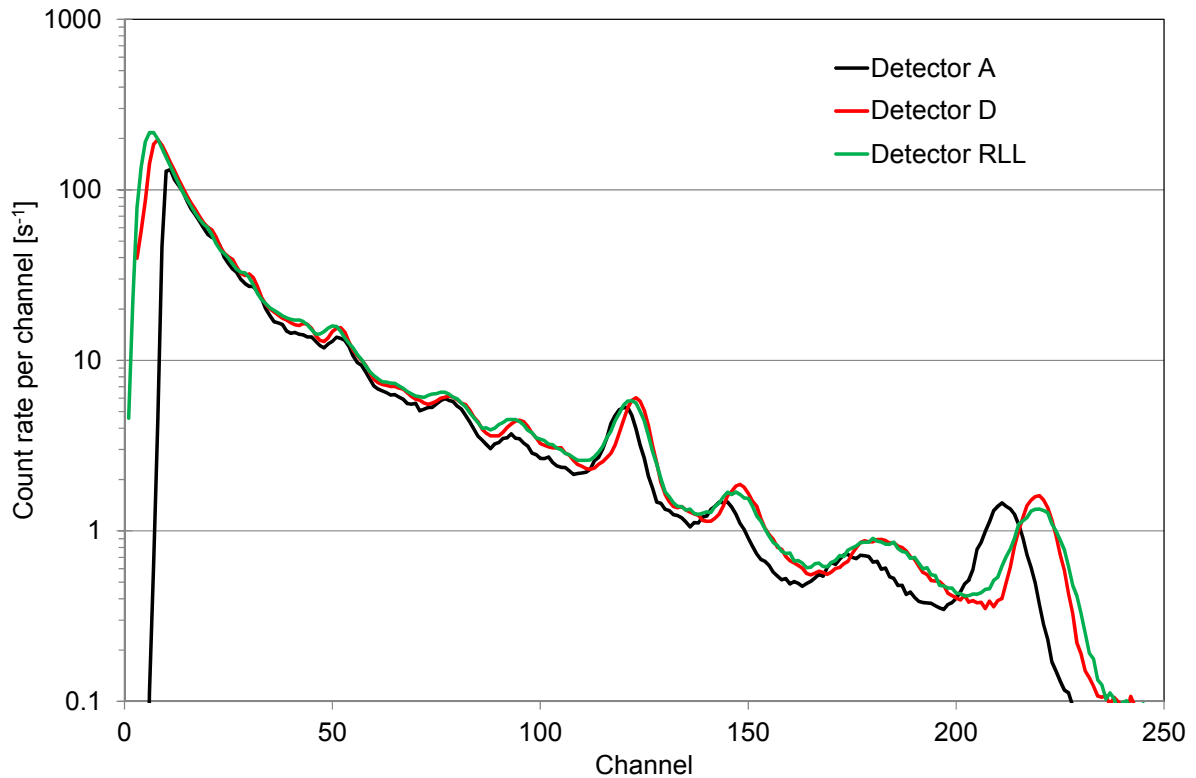


Figure 17: Comparison of raw spectra averaged over the measuring area.

The area around PSI was chosen for the intercomparison because of a known Thorium anomaly at Rotbergeg and photon emissions from facilities on the institute premises were expected to render sufficient data for the intercomparison. For the intercomparison, two radioactive sources were placed additionally on site by radiation protection staff of PSI (Figure 18). During the measuring flights, the shielding of the accelerator facility had to be opened for maintenance purposes, changing the radiological situation between flights. This radiation source could therefore not be used in the intercomparison. In the storage building OAHC (Figure 18) activated components of the accelerator facilities are stored prior to processing for disposal.

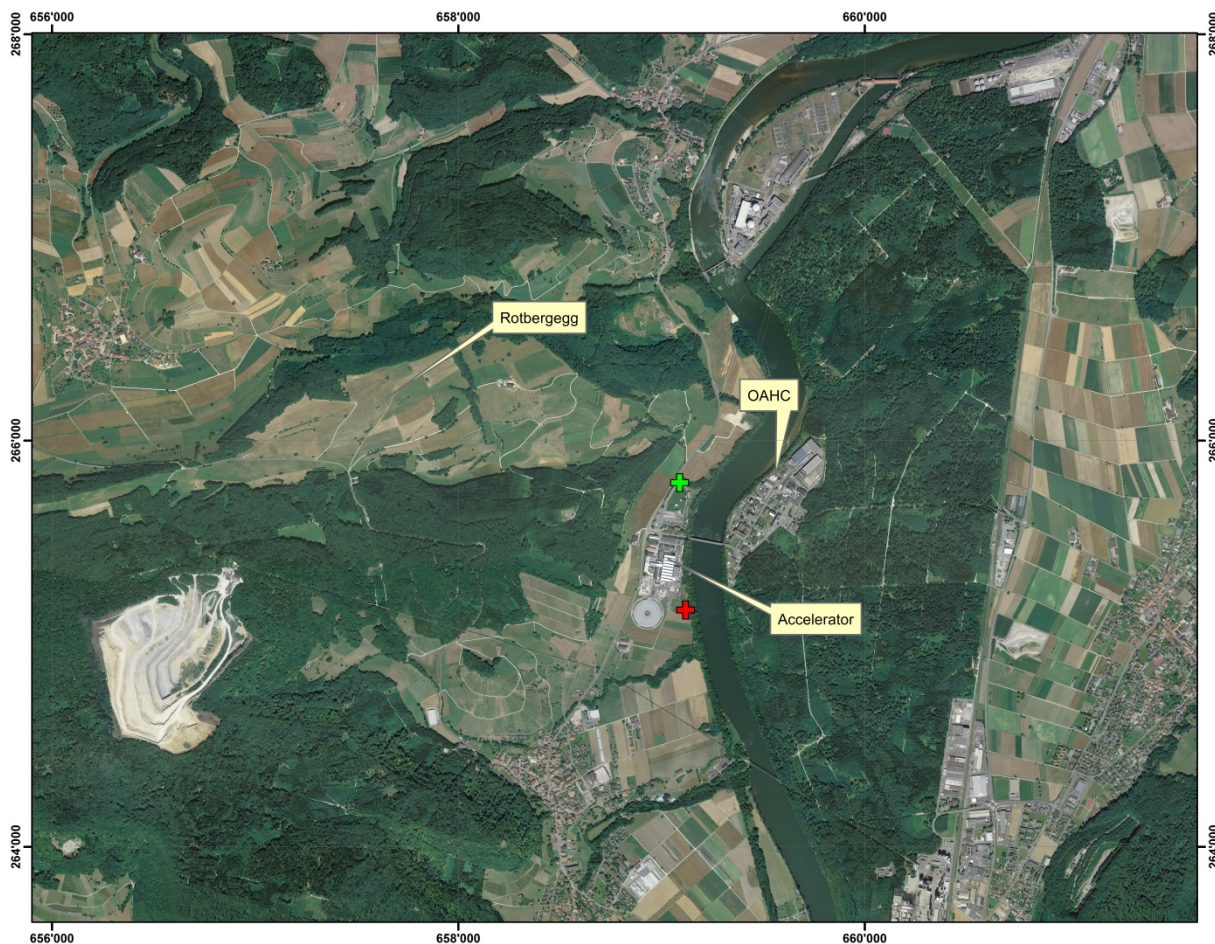


Figure 18: Aerial view of the intercomparison area. Source positions are marked with crosses (green - ^{137}Cs , red - ^{60}Co). swissimage25 © 2015 swisstopo (JD100042)

The comparison of results over the Thorium anomaly at Rotbergegg yields information on the general performance of the detectors, as the count rate of the Thorium energy window (Figure 3) does not have to be corrected for scattered photons of other radionuclide sources (see chapter 1.2).

The Thorium anomaly was detected with all three detectors. Figure 19 shows exemplarily the map of ^{232}Th activity concentration derived from the measuring flight with detector D.

The average activity concentrations in a rectangle over the anomaly between coordinates (657349, 266132) and (657794, 266336) were calculated for the comparison of the detectors and compared to ground measurements with in-situ gamma-spectrometry (Table 4). All values agree within the uncertainties estimated according to (Bucher, 2001). The ^{137}Cs activity concentration measured with in-situ gamma-spectrometry is just below the estimated detection limit of the airborne gamma-spectrometry system of 20 Bq/kg. The results indicate a possible over-correction of the influence of a Thorium-source into the Caesium energy window for detectors A and RLL, whereas an under-correction may be the case for detector D. The raw data obtained with detector RLL were evaluated using the parameters determined experimentally for detector D (see Chapter 1.2). As the calculated activity concentrations for detector RLL are the lowest in Table 4, about 20% lower efficiency of the prototype system may be conjectured.

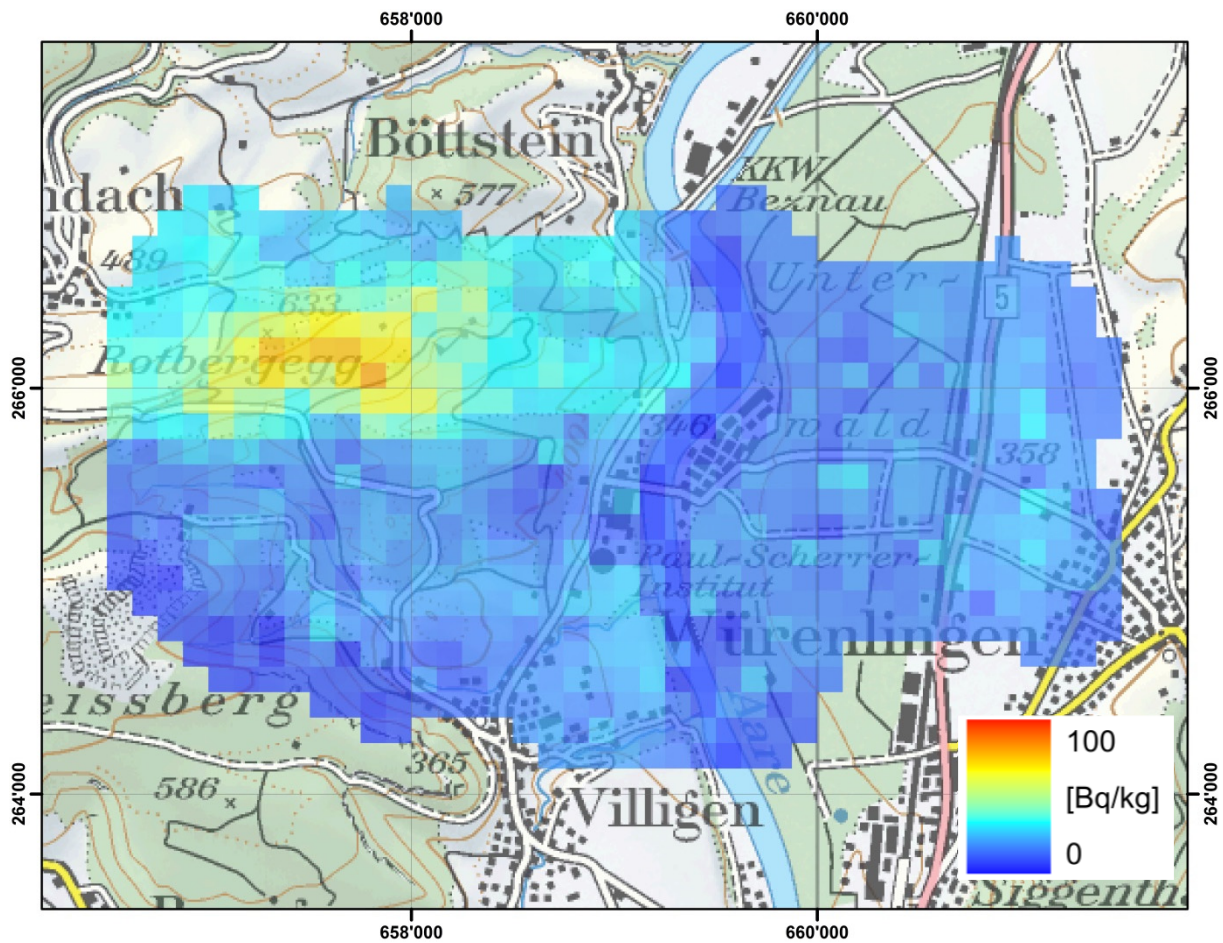


Figure 19: ^{232}Th activity concentration measured with detector D in the intercomparison area. PK100 © 2015 swisstopo (JD100042)

Table 4: Average activity concentrations over the Thorium anomaly at Rotbergegg

Nuclide	Activity concentration [Bq/kg]			
	Detector A	Detector D	Detector RLL	In-Situ
^{232}Th	83 ± 39	74 ± 34	60 ± 43	93 ± 17
^{137}Cs	9 ± 99	39 ± 86	2 ± 61	18 ± 3
^{40}K	220 ± 222	206 ± 199	158 ± 138	270 ± 45

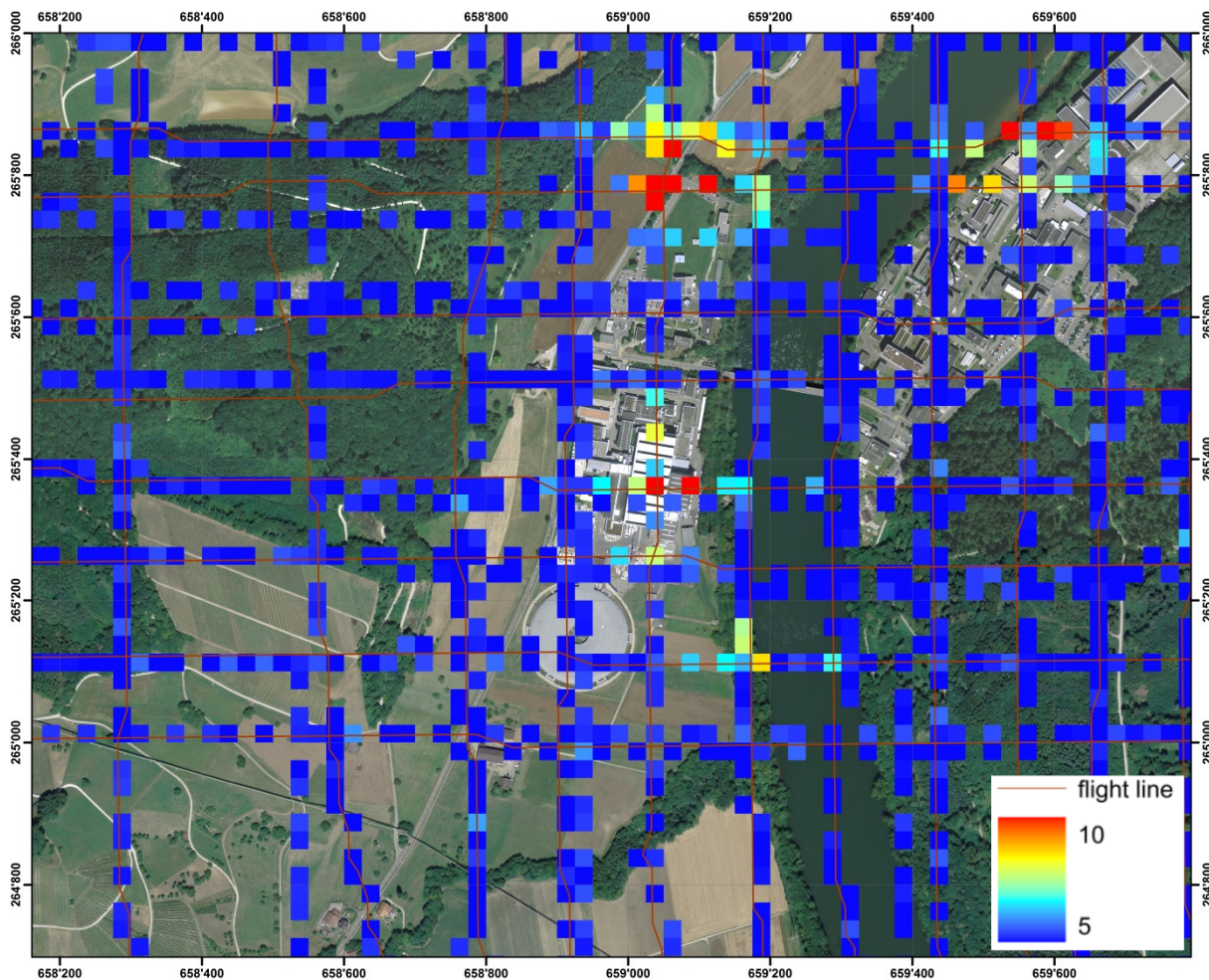


Figure 20: MMGC-ratio in the intercomparison area determined with detector RLL. swissimage25 © 2015 swisstopo (JD100042)

The radioactive sources placed on the institute premises, the accelerator facility and the storage building OAHC are identified on the map of the MMGC-ratio. Figure 20 shows exemplarily the MMGC ratio determined with detector RLL. The spectra measured over the building OAHC shows photons associated with the presence of ^{137}Cs and ^{60}Co (Figure 21). Ground measurements using in-situ gamma spectrometry found, that the stored components in OAHC contain only ^{60}Co and that the ^{137}Cs signal measured above OAHC has origins from two buildings adjacent to OAHC. The measurement was performed using two perpendicular sets of flightlines to study the influence of pitch and roll of the helicopter on the measurement result. No significant difference between the two flight directions (banding) was observed.

The point source activities calculated from the measured data are listed in Table 5 together with the activity of the known sources. From the data along the flight lines, the highest calculated activity in the vicinity of the source was selected. For the placed ^{137}Cs source, all three measuring system agree quite well, but underestimate the activity of the source. Detectors A and D continue to agree for all of the other sources of radiation, whereas Detector RLL shows much lower values. A possible reason may be a different positioning of the flight lines in the vicinity of building OAHC and the placed ^{60}Co -source.

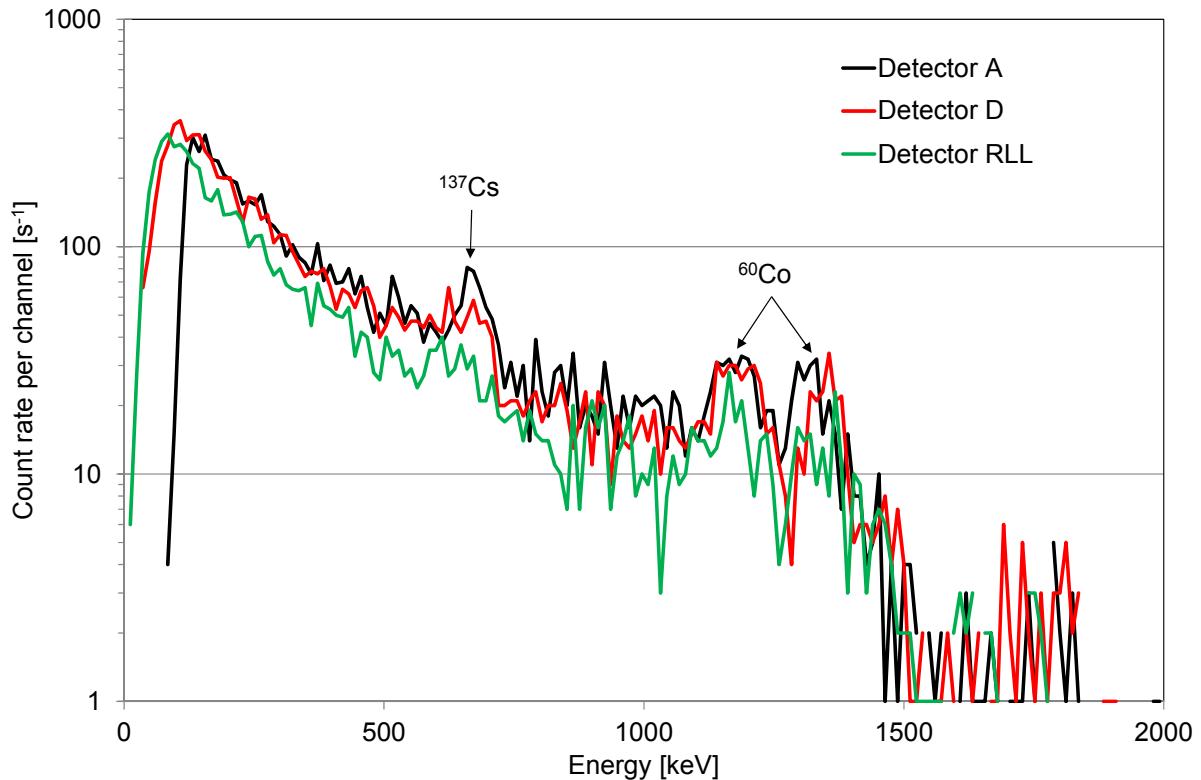


Figure 21: Photon spectra measured over the OAH building with three detectors.

Table 5: Source activities in the intercomparison area

Source	Activity [MBq]			Source
	Detector A	Detector D	Detector RLL	
OAH ^{60}Co	741 ± 232	772 ± 196	198 ± 315	-
OAH ^{137}Cs	1755 ± 658	1424 ± 527	358 ± 691	-
^{137}Cs placed	2583 ± 603	2646 ± 771	2585 ± 549	3562 ± 107
^{60}Co placed	291 ± 114	234 ± 109	101 ± 95	317 ± 10

2.5 Exercise RadEx14

Airborne gamma spectrometric measurements are only one tool in a response chain to a radiological emergency. The cooperation with ground measurements and first responders has to be trained besides exercising the ARM team itself. Integrated into the exercise ARM14 was a search and rescue exercise RadEx14 together with first responders of cantons Thurgau and Zurich. The exercise area was located near the city of Frauenfeld. The exercise area (red polygon in Figure 22) had a size of 175 m x 79 m, which is rather small compared to the field of view of the ARM detector (300 m x 300 m). In a real emergency, airborne gamma spectrometry would not be mobilised with the source location already known inside the field of view of the detector. Eleven ^{60}Co -sources with activities between 6 MBq and 41 MBq, totaling 317 MBq and two ^{137}Cs -sources with 1.8 GBq each were placed in five positions in the exercise area.

The main indicator for the presence of manmade radionuclides (MMGC-ratio) shows elevated values throughout the exercise area (Figure 23). The maximum values of point source activities determined over the measuring area were 251 ± 202 MBq for ^{60}Co and 3.1 ± 2.2 GBq for ^{137}Cs . This corresponds to 79% and 86% of the summed source activities placed in the exercise area of ^{60}Co and ^{137}Cs , respectively. This result could be expected as the maximum source distance of 91 m is well below the spatial resolution of the airborne gamma spectrometry system leading to superposition of photons from all placed sources in the detector.

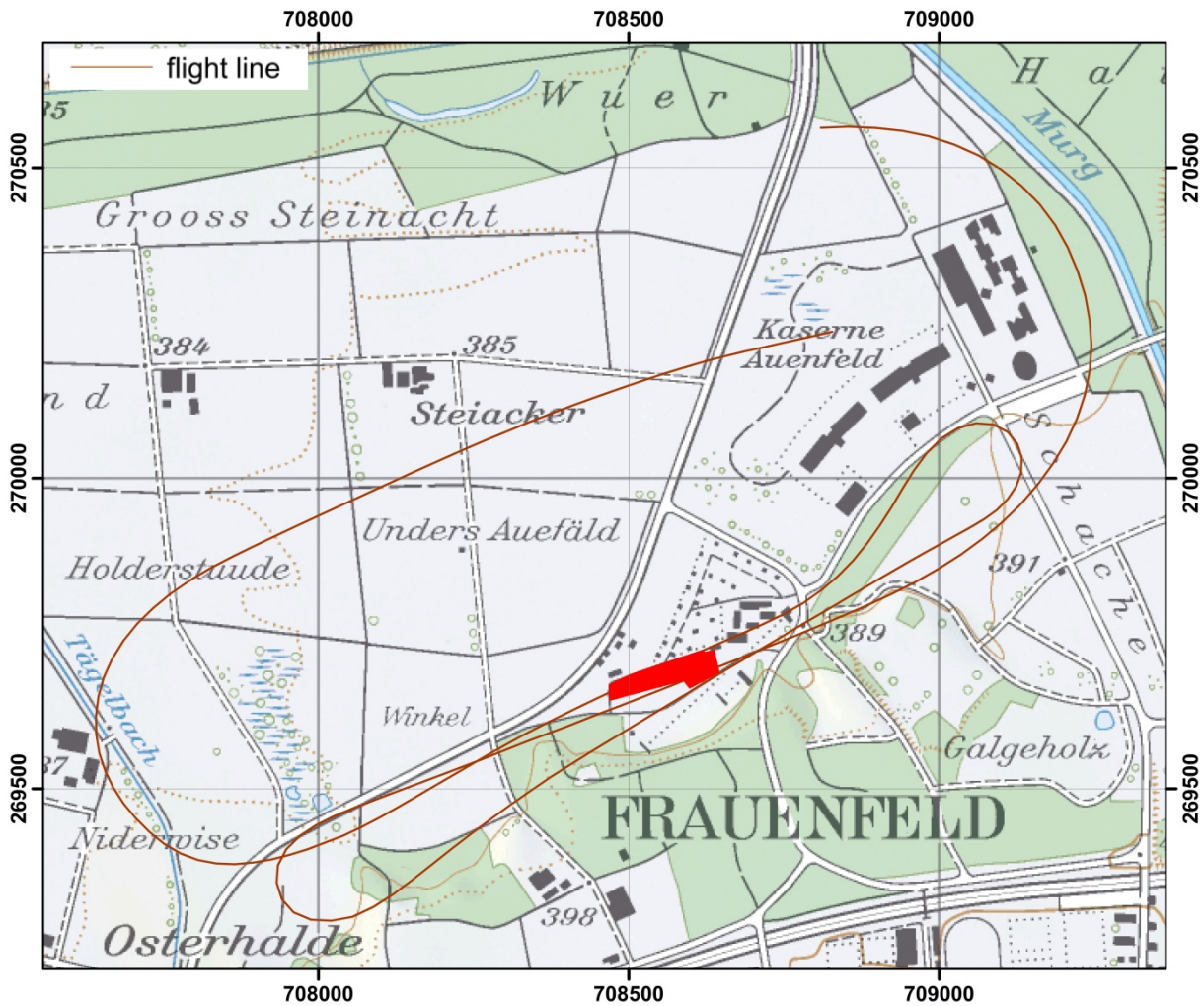


Figure 22: Flight lines and location of the exercise area near Frauenfeld. PK25
© 2015 swisstopo (JD100042)

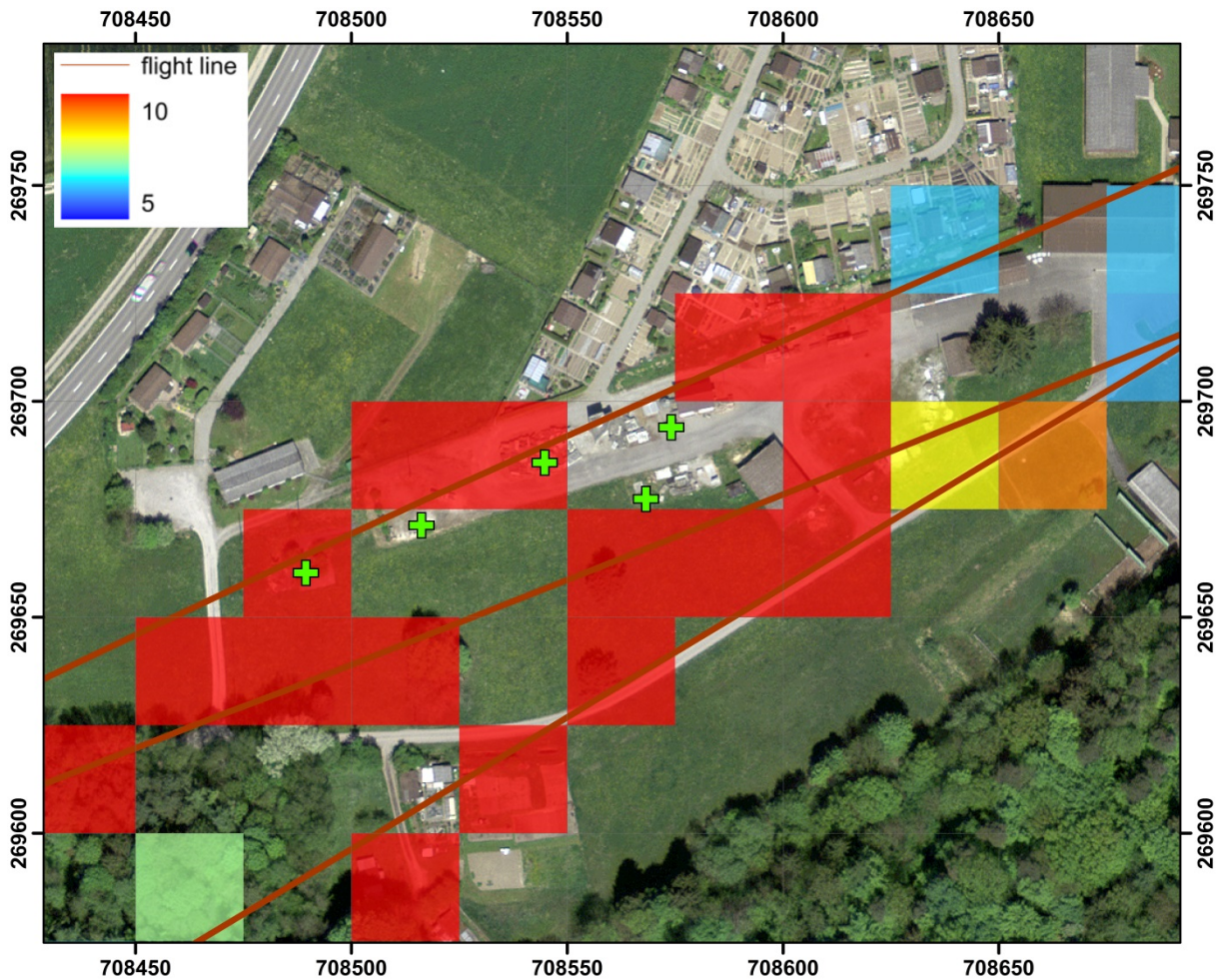


Figure 23: MMGC-ratio in the exercise area. Source positions are marked with green crosses. swissimage25 © 2015 swisstopo (JD100042)

2.6 Exercise FTX14

The NEOC participated between November 10th and 18th in the exercise FTX14 of 900 Swiss and German military ABC and EOD personnel in the vicinity of Geneva with the airborne gamma spectrometry equipment. The exercise included a search for radioactive sources near Bière in the canton Vaud. Compared to the exercise RadEx14 in the previous chapter, the scenario and size of the exercise area were more realistic for a deployment of the airborne gamma spectrometry system. Seven radioactive sources were placed by in the exercise area (Table 6 and Figure 24). With the exception of the inhabited regions of the exercise area, practically the whole exercise area is more or less influenced by the sources. Thus, locating an appropriate background area for spectrum comparison was virtually impossible. The source spectra (Figure 27, Figure 28, Figure 30, Figure 32 and Figure 33) are therefore depicted without a reference background spectrum.

Table 6: Radioactive sources in the exercise area and measured activities.

Nuclide	Source Activity [GBq]	Coordinate		Measured activity [GBq]
		x [m]	y[m]	
^{137}Cs	49	515073	153391	52 ± 26
^{137}Cs	9.8	515317	153236	11 ± 10
^{137}Cs	9.8	514051	153928	12 ± 13
^{137}Cs	0.9	515413	152867	1.1 ± 1.8
^{60}Co	0.5	515172	153382	0.6 ± 0.3
^{133}Ba	0.7	515332	152896	-
^{241}Am	1.8	516152	152989	-

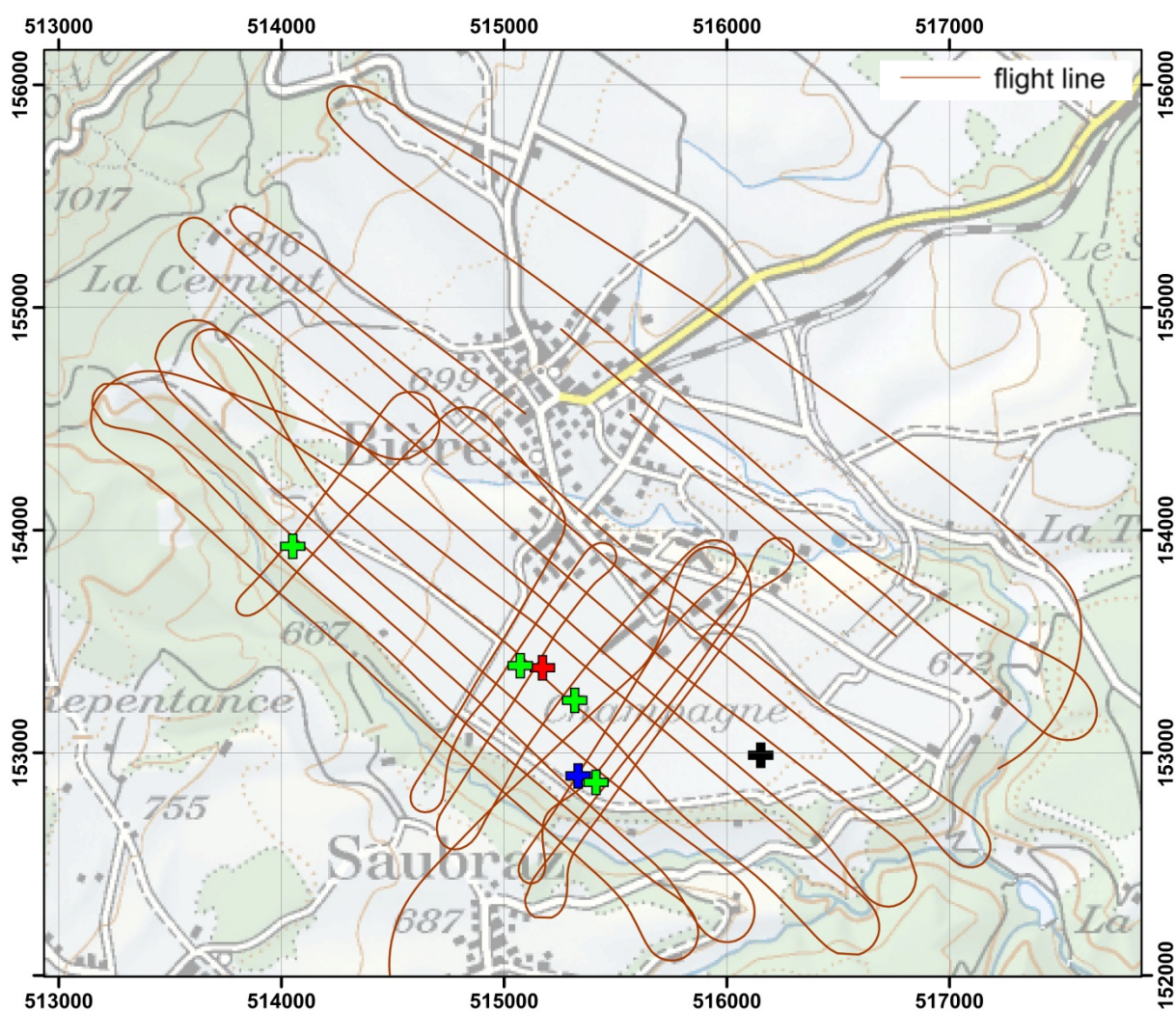


Figure 24: Positions of the radioactive sources in the exercise area (crosses; green - ^{137}Cs , red - ^{60}Co , blue - ^{133}Ba , black - ^{241}Am). PK100 © 2015 swisstopo (JD100042)

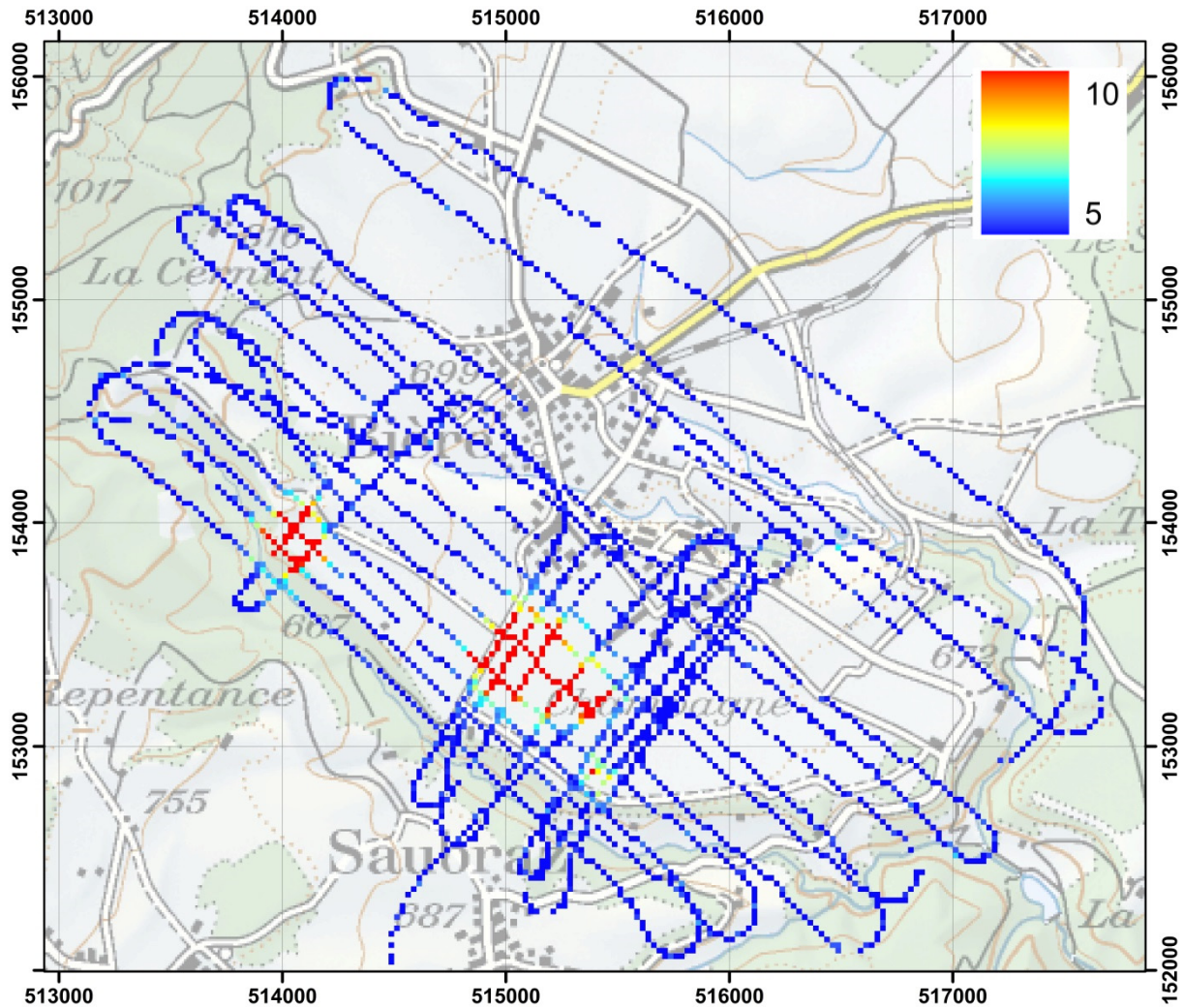


Figure 25: MMGC-ratio in the exercise area. PK100 © 2015 swisstopo (JD100042)

The map of the MMGC-ratio (Figure 25) shows clearly three distinct areas with suspected man-made radionuclides covering six of the placed sources.

The location of the ^{241}Am -source is not identified. As the MMGC-ratio does not consider photon emissions below 400 keV, the photon emission of ^{241}Am with energy 60 keV does not increase this parameter.

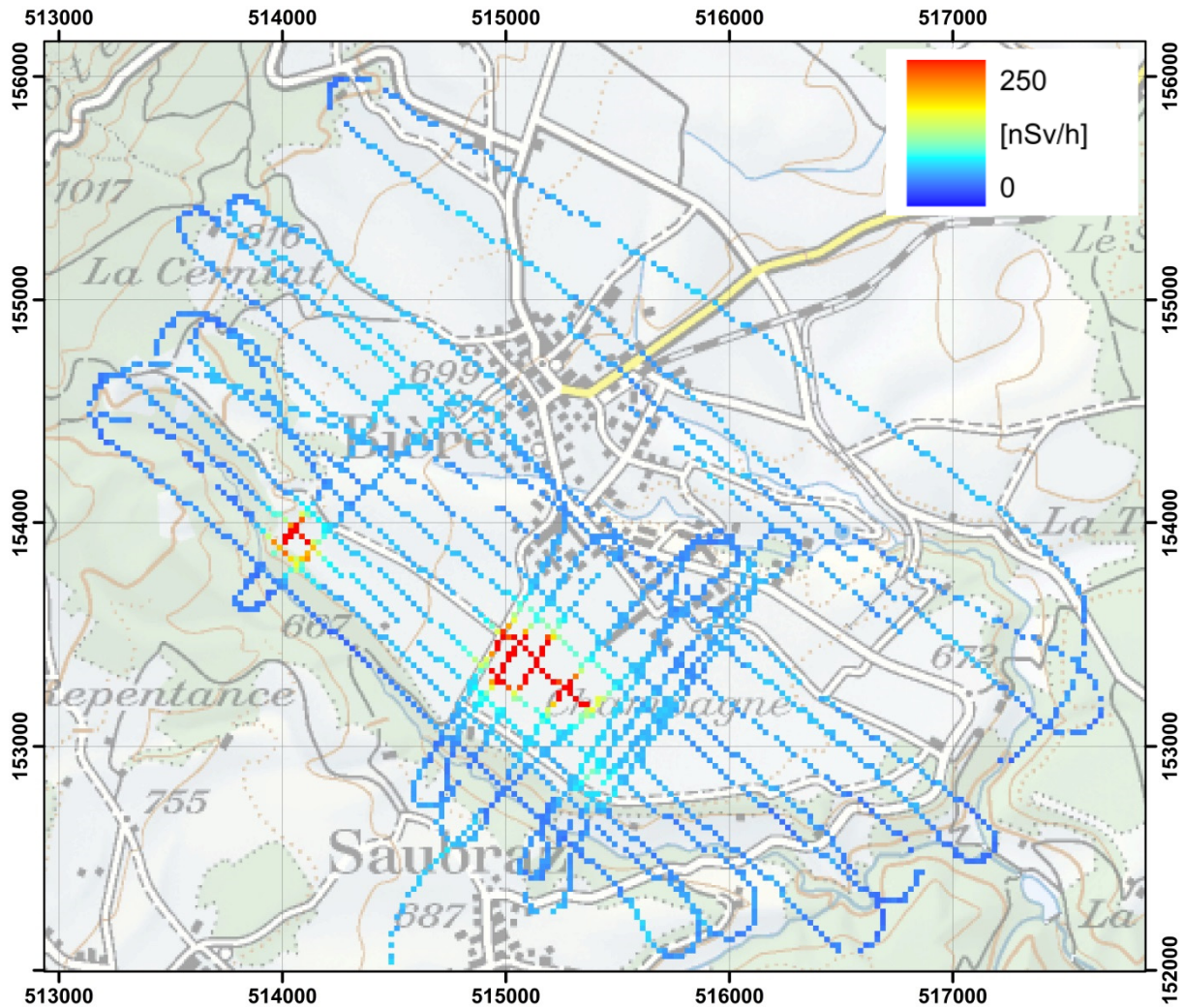


Figure 26: Terrestrial component of the dose rate in the exercise area. PK100 © 2015 swisstopo (JD100042)

The photon radiation at 60 keV would not register in the map of the terrestrial dose rate (Figure 26) calculated with the Spectrum Dose Index (SDI) method as the algorithm to calculate the SDI considers only photons above an energy of 240 keV.

The photon spectrum at the measuring point nearest to the ^{241}Am -source (Figure 27) shows a slight signal of the 60 keV radiation on the low-energy slope of the spectrum. Even a skilled operator of the airborne gamma spectrometry system would not have detected such a slight signal without information on the location and the radionuclide of the source.

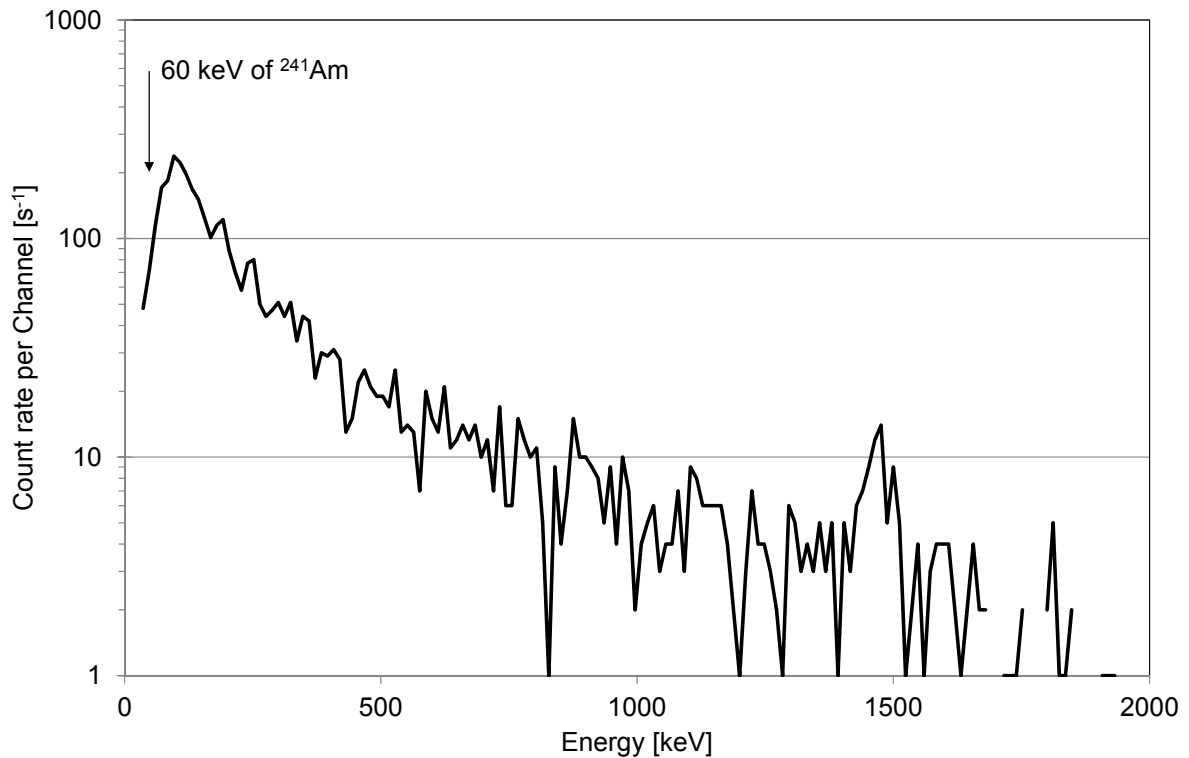


Figure 27: Photon spectrum measured near the ²⁴¹Am-source.

The area around coordinate (515426, 152888) with suspected man-made radionuclides indicated in the MMGC-ratio map (Figure 25) contains both a ¹³⁷Cs-source and the ¹³³Ba-source. A next step of the ARM-operator would be the nuclide identification using a photon spectrum averaged over the indicated area (Figure 28). The signal from 662 keV photons is clearly visible in the averaged spectrum, whereas the signal originating from the ¹³³Ba-source with photons of energies 302 keV, 356 keV and 384 keV is less pronounced. In such a case, the identification of the ¹³³Ba-source during the flight depends largely on the skill and experience of the ARM-operator.

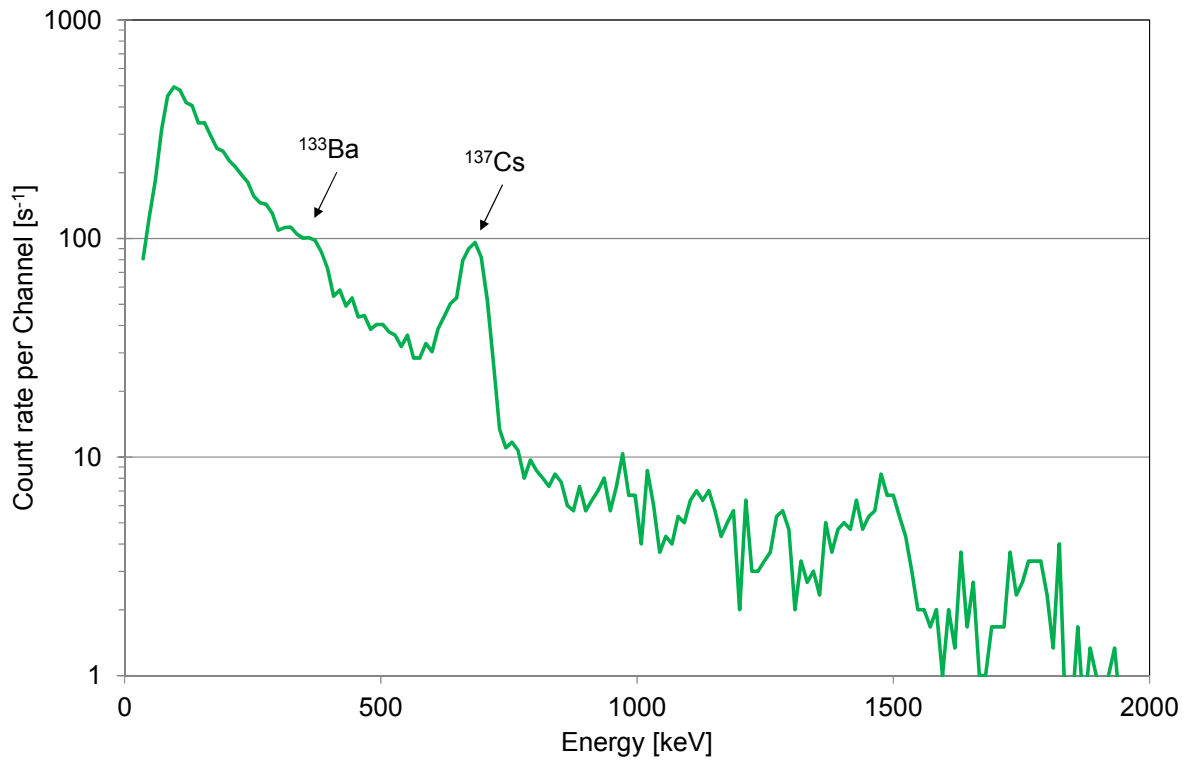


Figure 28: Photon spectrum averaged over the indicated area around coordinate (515426, 152888).

The detection of the ¹³⁷Cs-source is verified in a third step using the map of ¹³⁷Cs-point-source activity (Figure 29), which clearly shows a signal with an estimated source activity of 1.1 ± 1.8 GBq.

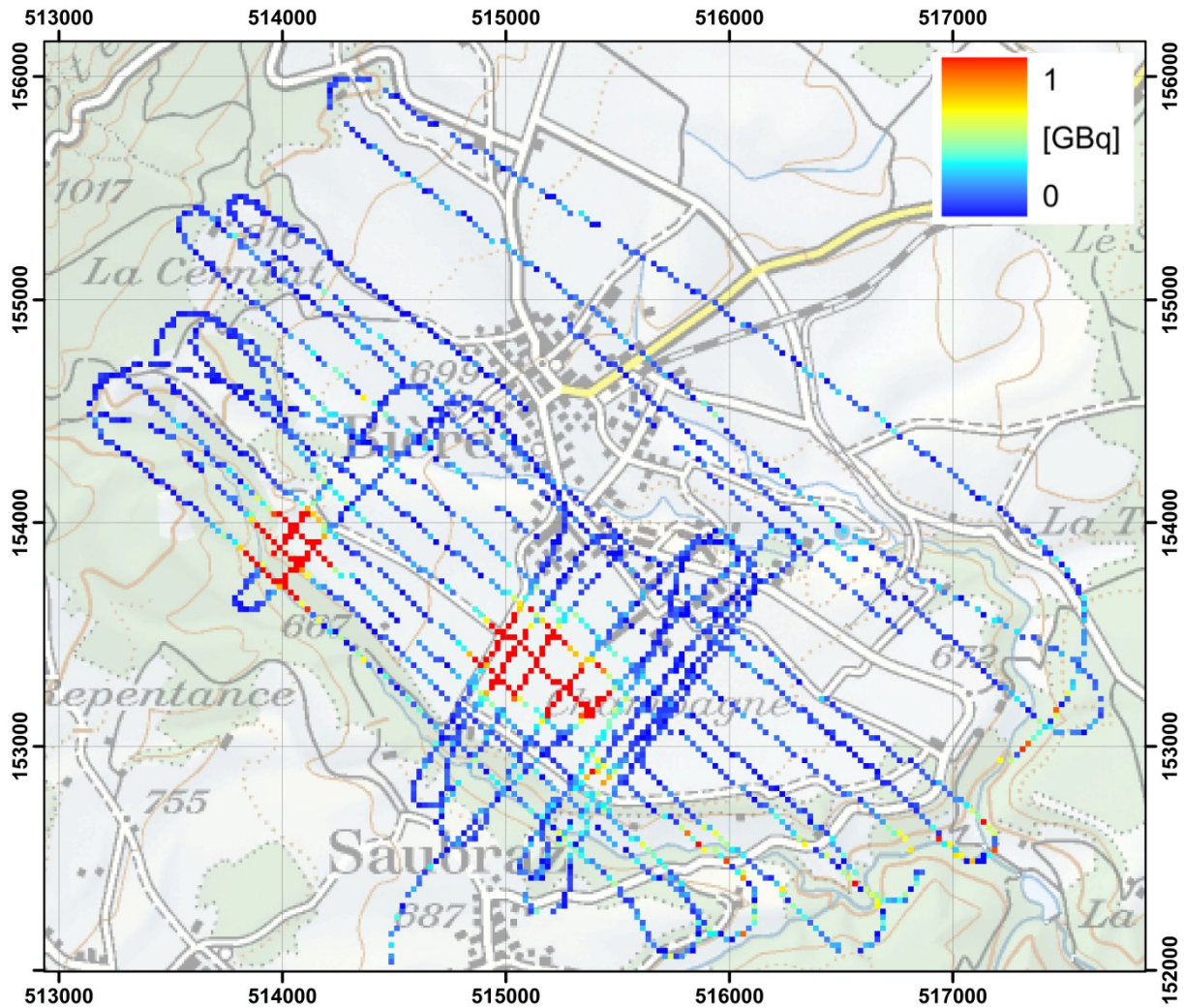


Figure 29: Estimated ^{137}Cs -point-source activity in the exercise area. PK100 © 2015 swisstopo (JD100042)

The average photon spectrum over the indicated area at coordinate (514055, 153909) shows clearly a signal of the 662 keV photon emission of ^{137}Cs (Figure 30). The spectral information is confirmed in the map of the ^{137}Cs -point source activity (Figure 29) with an estimated source activity of 12 ± 13 GBq at the measuring point next to the source location.

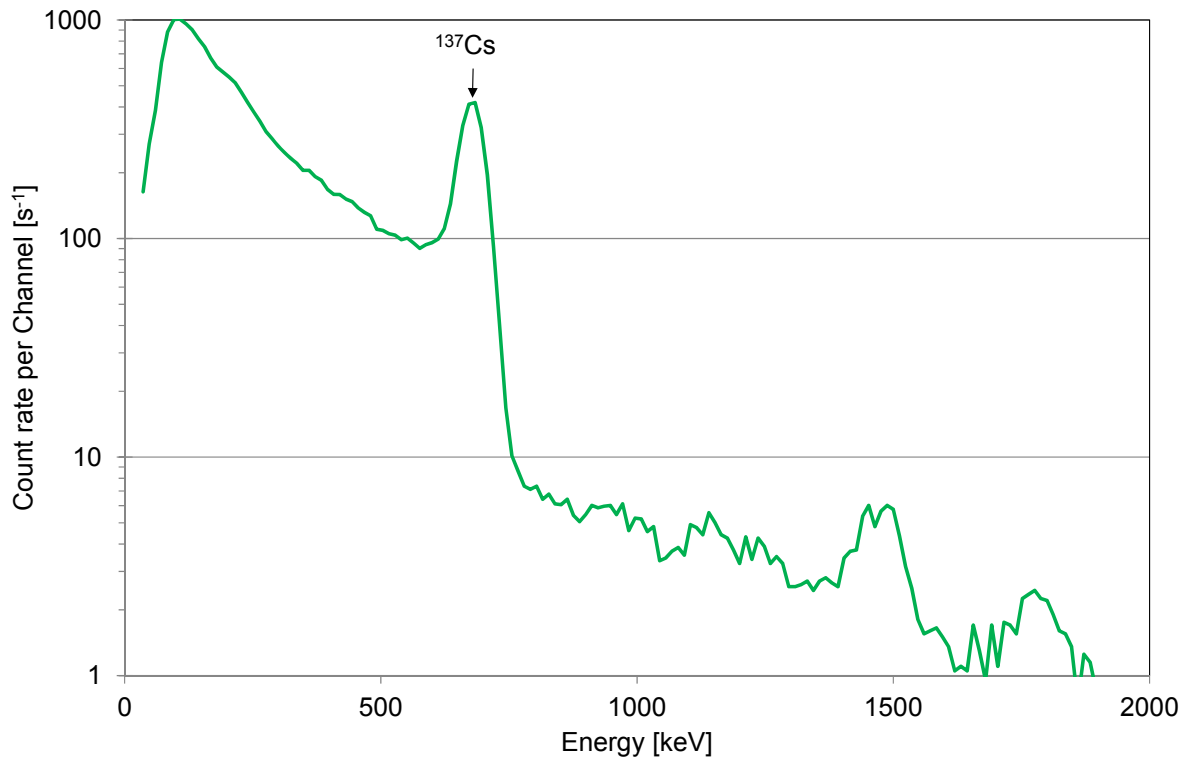


Figure 30: Photon spectrum averaged over the indicated area around coordinate (514055, 153909).

The elongated shape of the third area around coordinate (515164, 153342) indicated in the map of the MMGC-ratio (Figure 25) gives a first hint on the presence of more than one radioactive source. A rescaling of the MMGC-ratio map splits the area into two locations of suspected radioactive sources (Figure 31). The average spectrum over the first location around coordinate (515289, 153239) depicts again the typical spectrum of a ^{137}Cs -source. The estimated ^{137}Cs -point-source activity of 5 GBq at the measuring point next to the source position (Table 6) is not the largest observed in the suspected area. The largest estimated ^{137}Cs -point-source activity of 11 ± 10 GBq was measured at coordinate (515291, 153237) at a distance of 26 m from the specified source position.

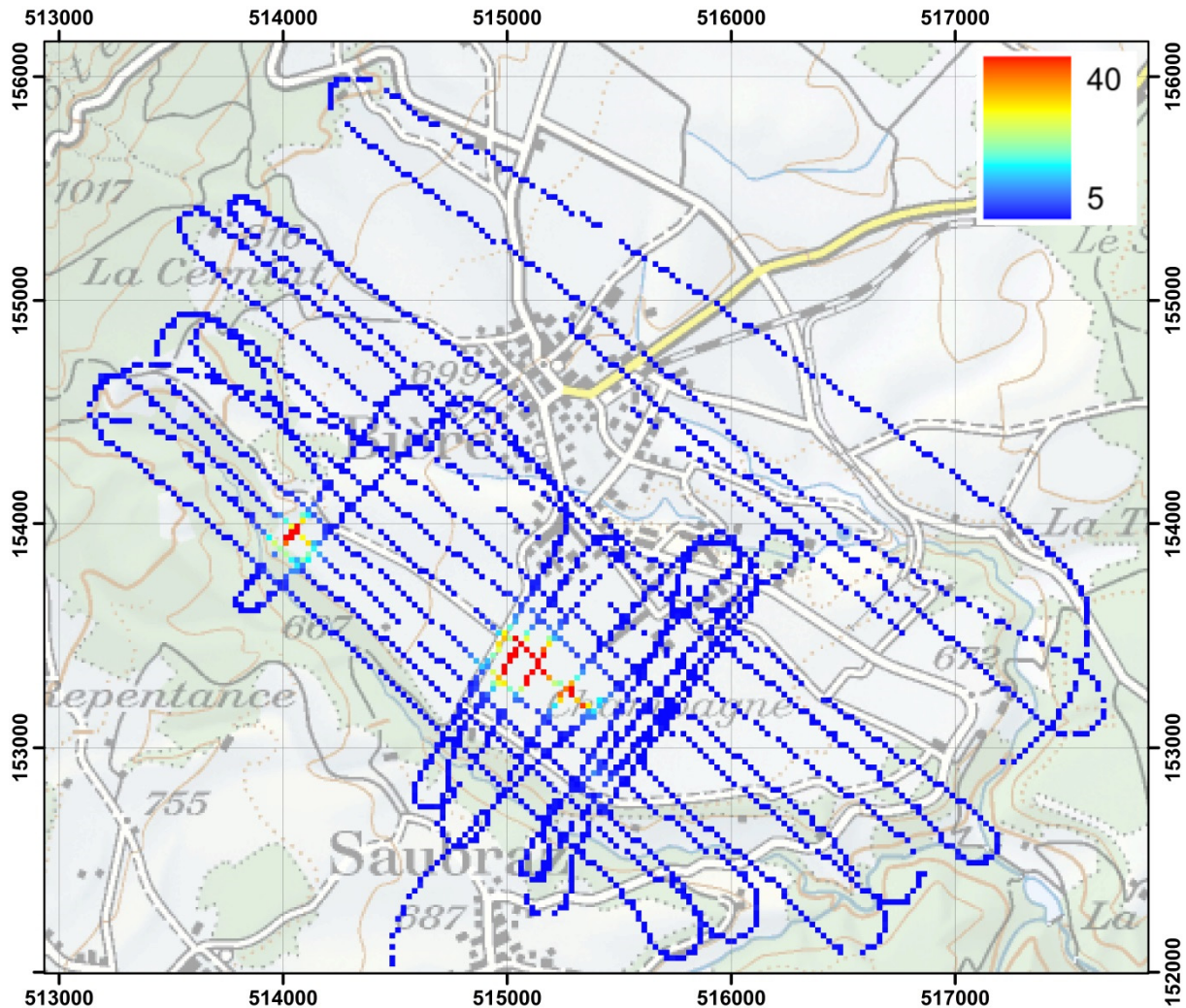


Figure 31: Rescaled MMGC-ratio in the exercise area. PK100 © 2015 swisstopo (JD100042)

The photon spectrum averaged over the remaining area of suspected man-made radionuclides around coordinate (515071, 153398) shows besides a very large signal of the 662 keV photon emission of ^{137}Cs two additional peaks at energies of 1173 keV and 1332 keV, which are associated with the radionuclide ^{60}Co (Figure 33). This observation is confirmed in the map of ^{60}Co -point source activity (Figure 34). Again, the maximum ^{60}Co -point-source activity of 0.6 ± 0.3 GBq is not found at the measuring point nearest to the provided source position, but at a point 39 m away. In contrast, the maximum value of the estimated ^{137}Cs -point-source activity of 52 ± 26 GBq was found at the measuring point next to the specified source position.

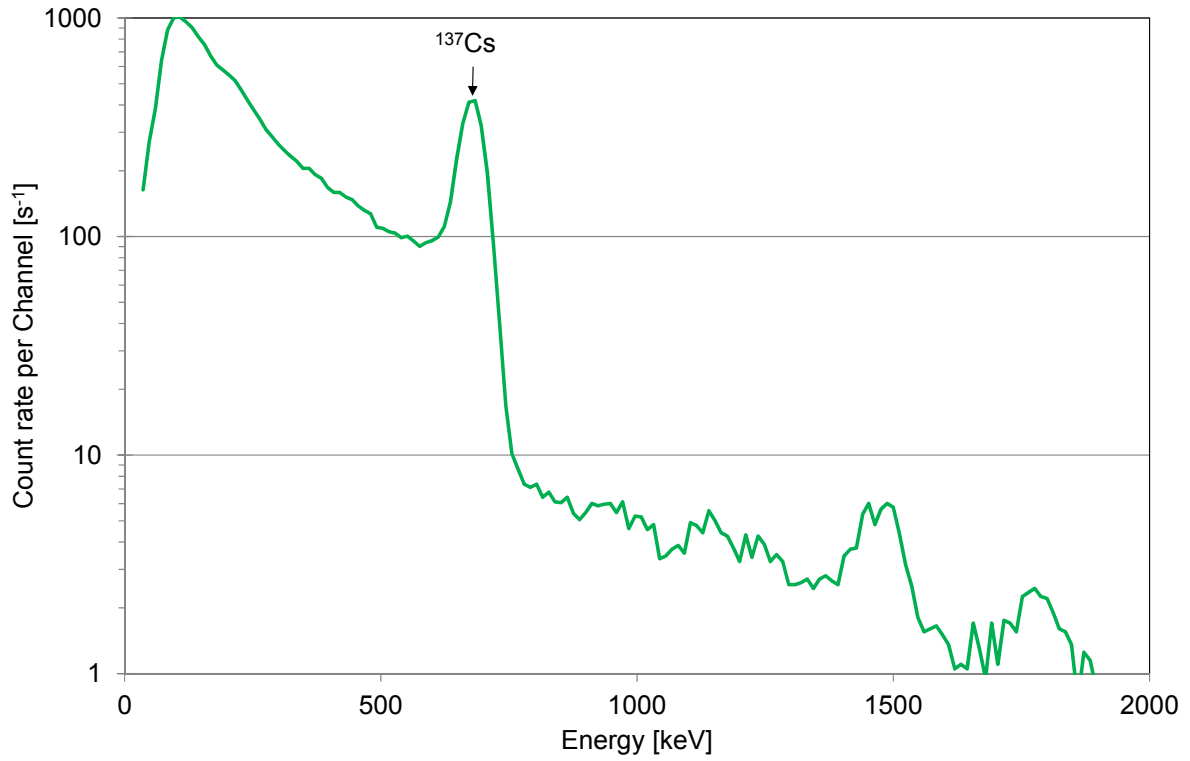


Figure 32: Photon spectrum averaged over the indicated area around coordinate (515289, 153239).

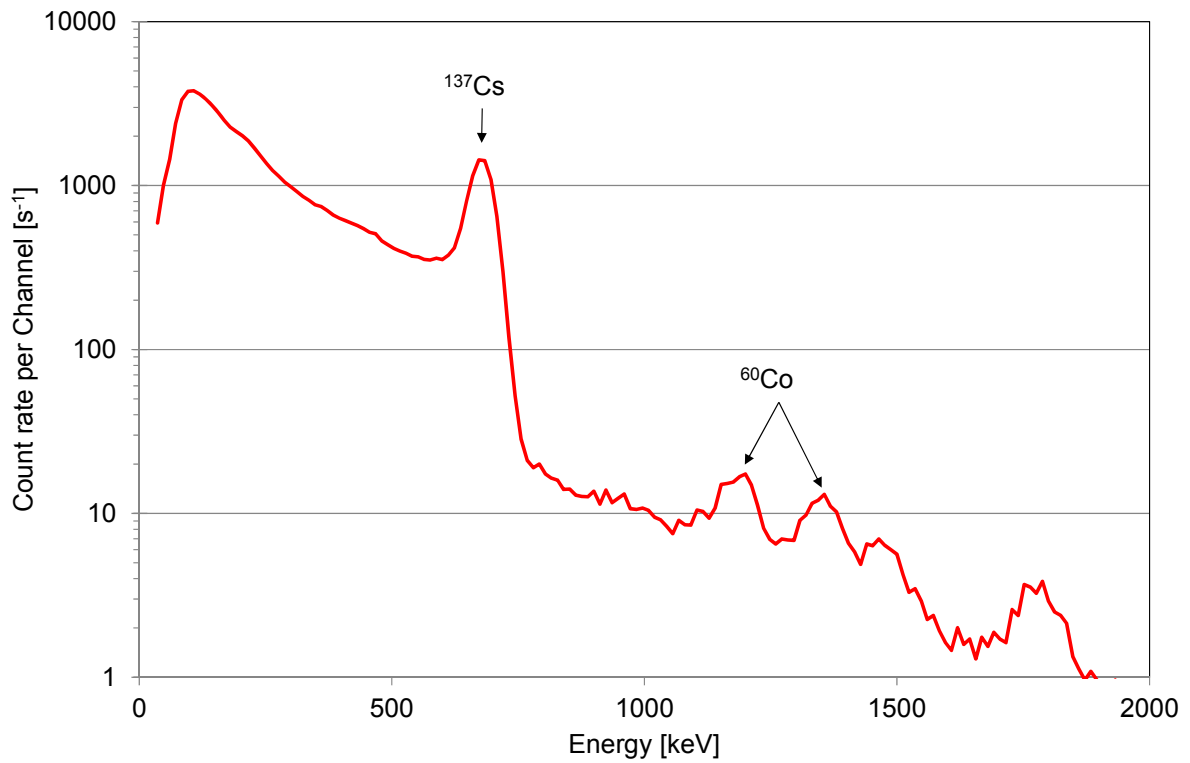


Figure 33: Photon spectrum averaged over the indicated area around coordinate (515071, 153398).

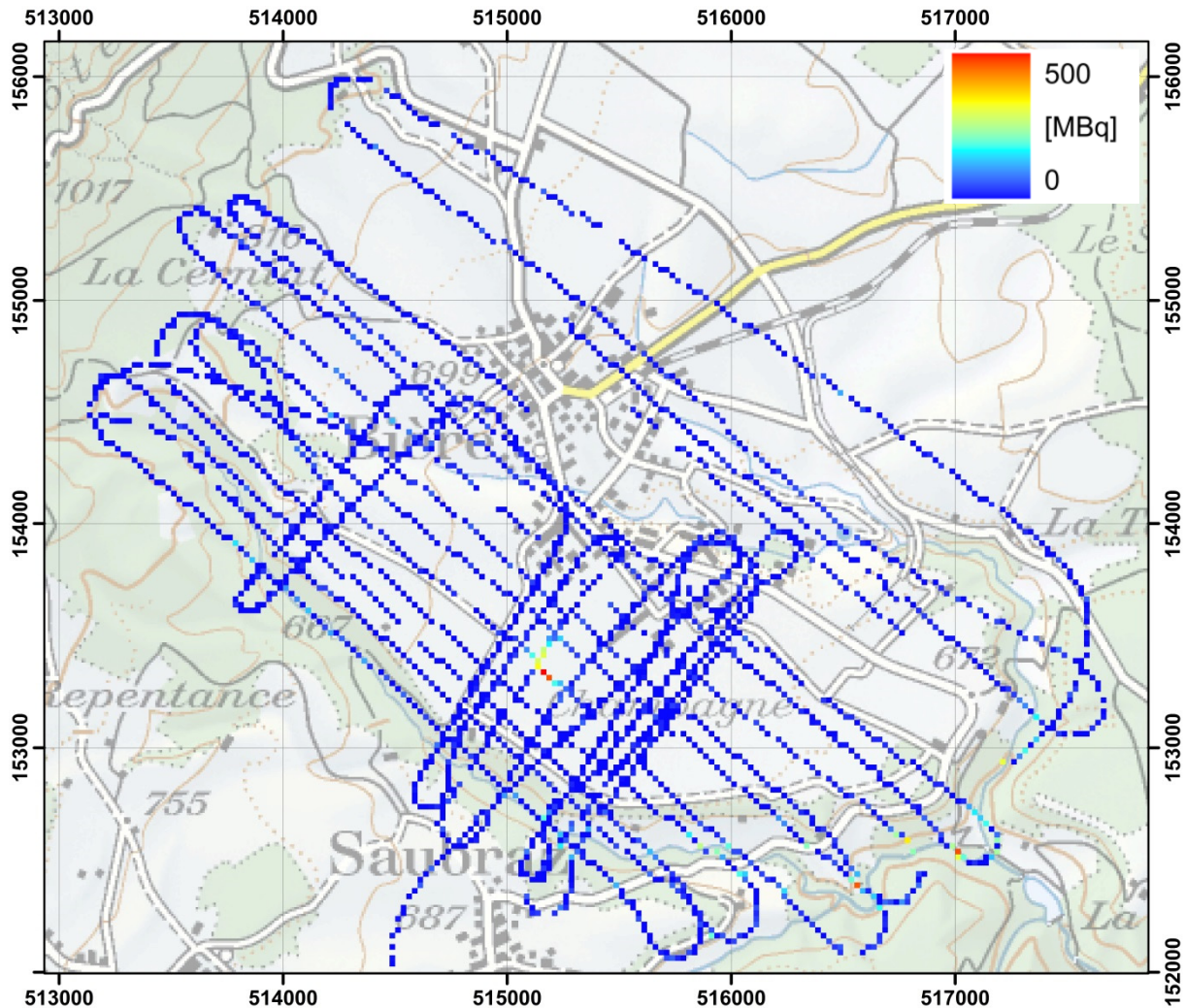


Figure 34: Estimated ^{60}Co -point-source activity in the exercise area. PK100 © 2015 swisstopo (JD100042)

2.7 Profile St. Gallen - Maloja

For the extension of Swiss radiological maps, a profile was measured from St. Gallen to Maloja. Figure 35 shows the path chosen for the measurement. The length of the flight path is measured starting at the St. Gallen entry point and this length is used as ordinate for Figure 36 and Figure 37. The terrestrial component of the dose rate (Figure 36) along the flight path shows low values where photon emissions of the ground are attenuated by water. The terrestrial dose rate is further influenced by the presence of natural radionuclides. For example, the increased terrestrial dose rate 82 km along the flight path can be clearly associated with an elevation of the ^{232}Th activity concentration (Figure 37).

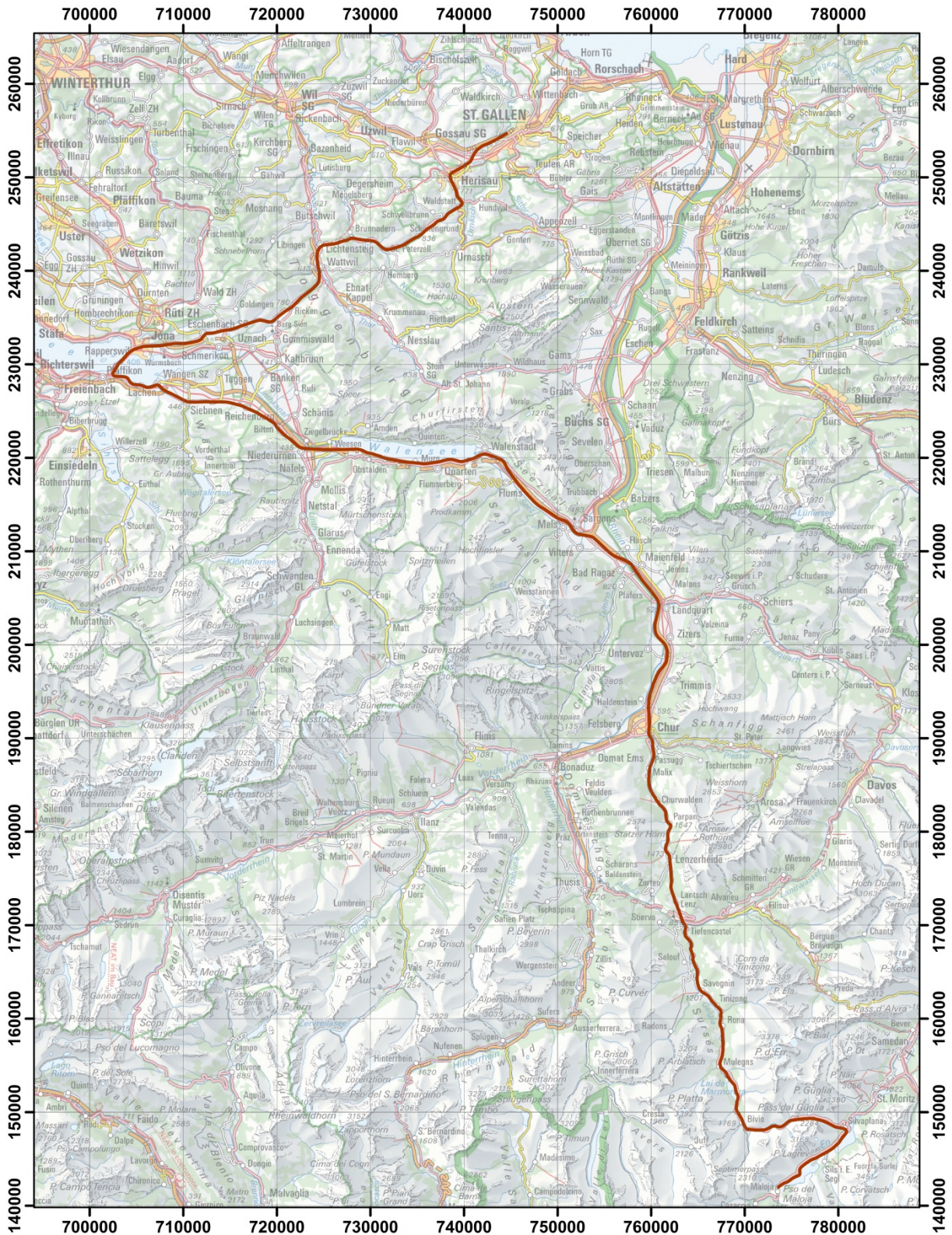


Figure 35: Flight line of the profile from St. Gallen to Maloja. PK500 © 2015 swisstopo (JD100042)

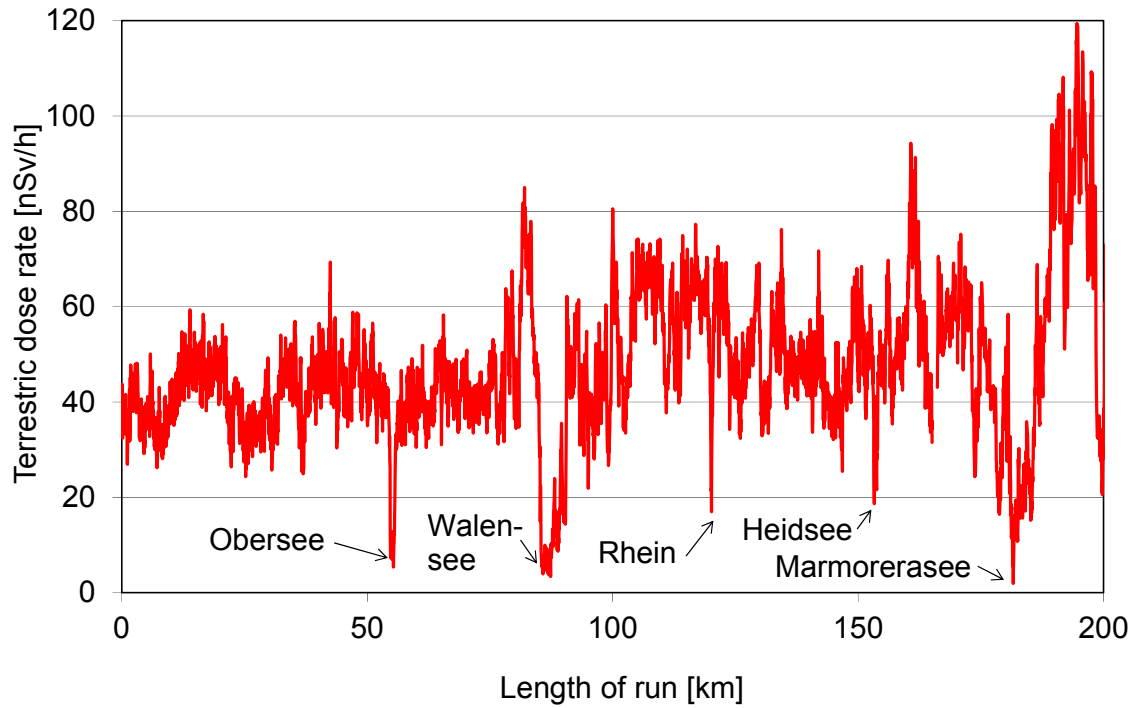


Figure 36: Terrestrial dose rate along the profile from St. Gallen to Maloja.

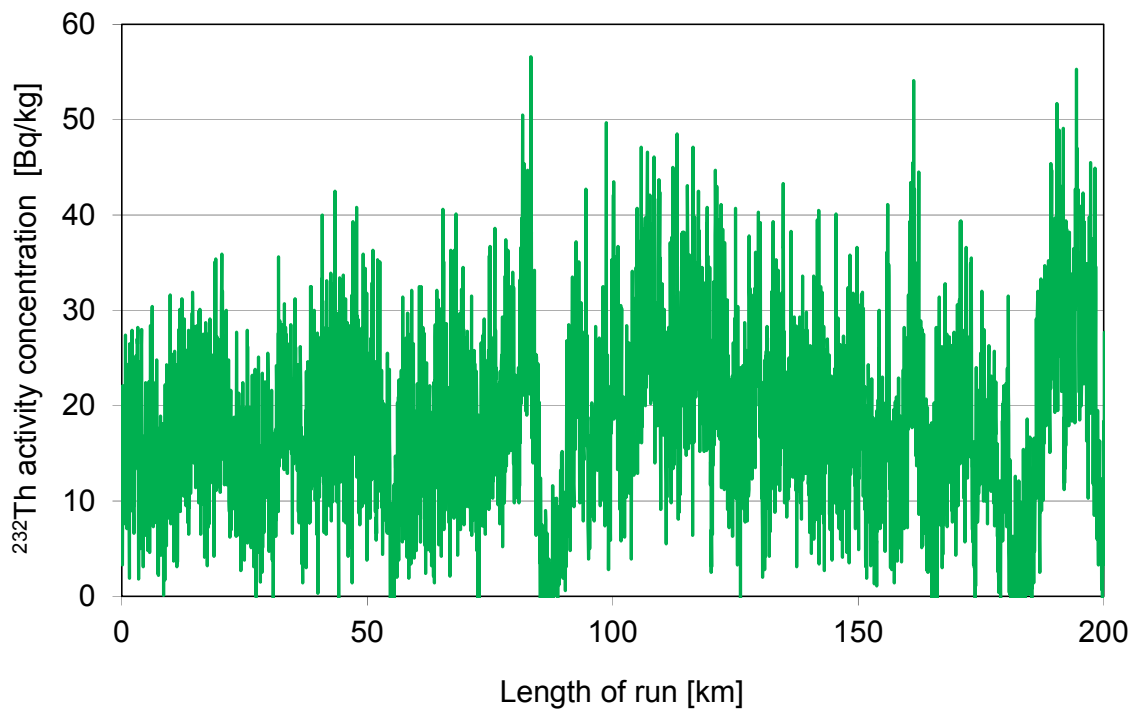


Figure 37: ^{232}Th activity concentration along the profile from St. Gallen to Maloja.

2.8 Profile Koppigen - Zurich

For the extension of Swiss radiological maps, a profile was measured from Koppigen to Zurich on the return flight from the exercise FTX14. Figure 35 shows the path chosen for the measurement. Low values of the terrestrial component of the dose rate (Figure 39) along the profile are usually encountered where photon emissions of the ground are attenuated by water. Such a correlation can only be made for the minimum at 73 km of the run, which is associated with Lake Zurich. Other minima do not correspond to rivers or lakes. This indicates possible artefacts in the data evaluation process. Source of these artefacts is the average flight altitude of 331 m used during the measurement of the profile. In this altitude, the raw signal from ground radionuclides is reduced by a factor of 10 compared to the standard flight altitude of 100 m due to the square law and the probability of statistical artifacts is increased accordingly. On the other hand, a comparison with the large variation of heights above ground along the flight path (Figure 40) demonstrates the quality of the altitude correction algorithm used in the data evaluation.

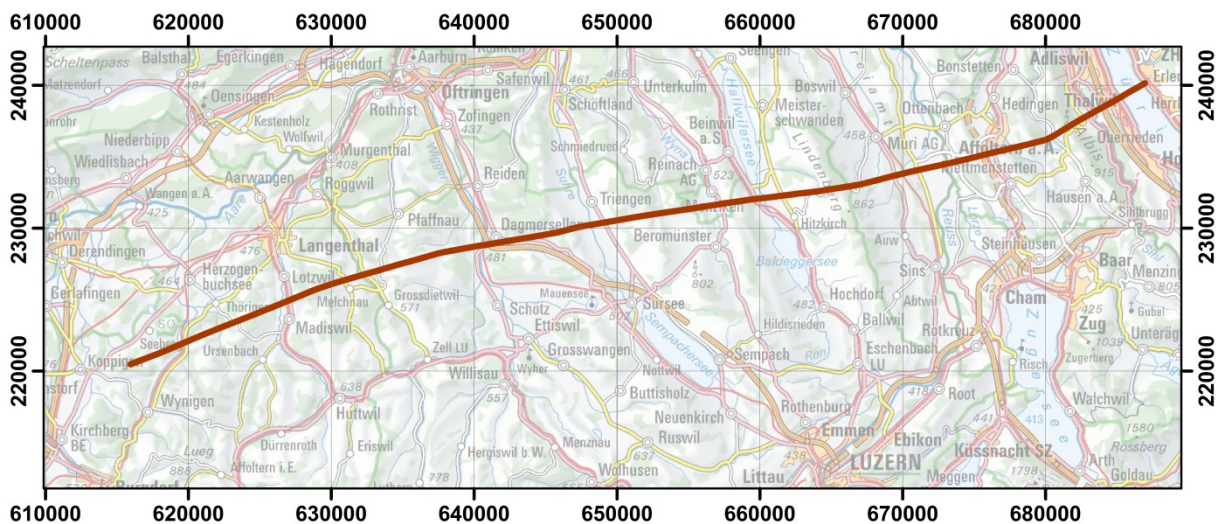


Figure 38: Flight line of the profile from Koppigen to Zurich. PK500 © 2015 swisstopo (JD100042)

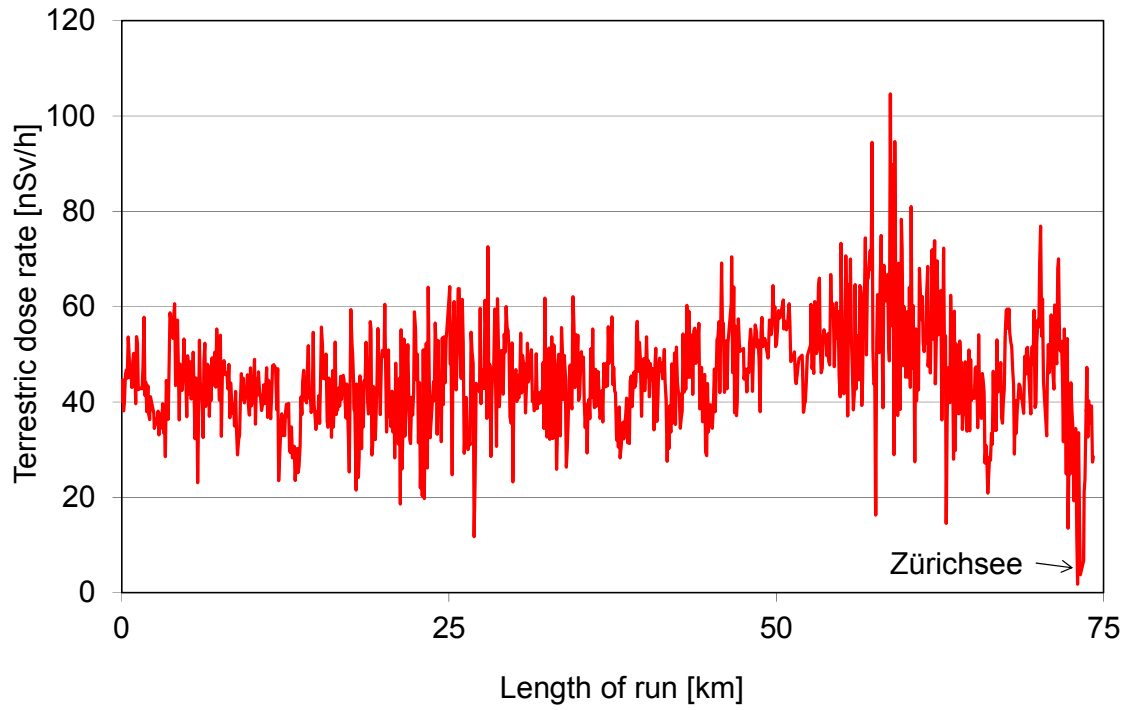


Figure 39: Terrestrial dose rate along the profile from Koppigen to Zurich.

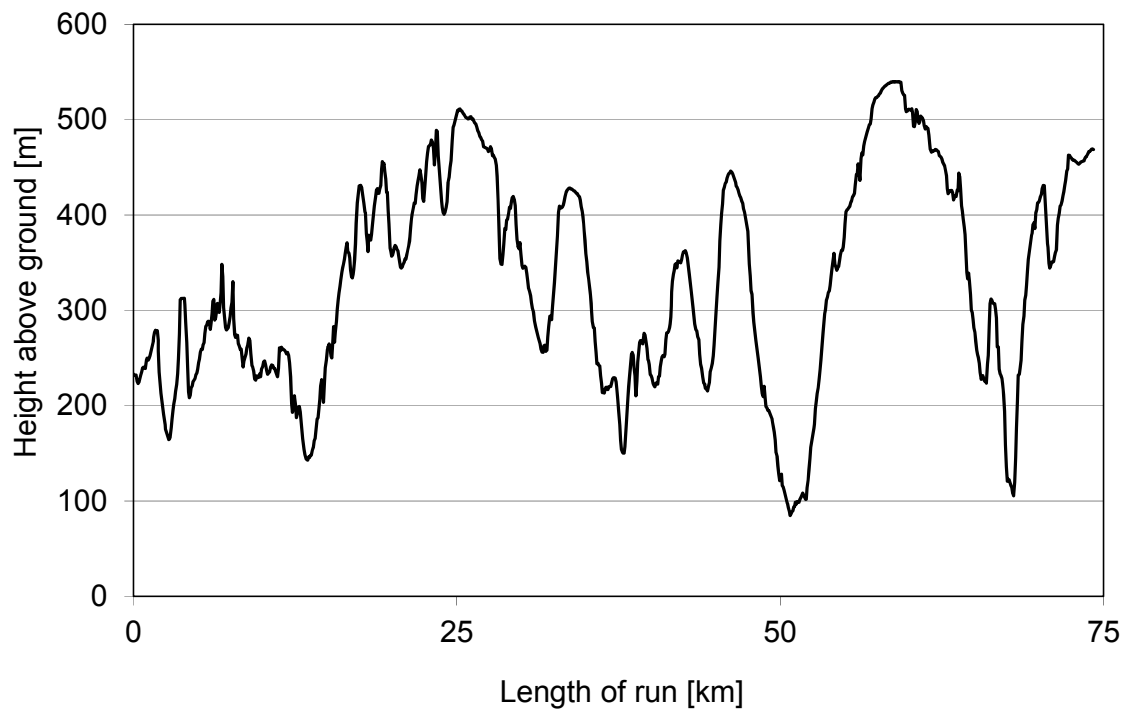


Figure 40: Height above ground along the profile from Koppigen to Zurich.

3 CONCLUSIONS

A new detector (detector D) was characterised in the laboratory and the according parameter file for data evaluation generated. In this context, the characterisation measurements performed in 2007 for detector A and C were re-evaluated to improve consistency between the different parameter sets.

The measurement over the nuclear power plants Beznau (KKB) and Leibstadt (KKL), the Paul Scherrer Institute and the intermediate storage facility ZWILAG following a bi-annual routine showed no artificial radionuclides outside of the plant premises. As in previous years, the distinction between pressurized and boiling water reactor is clearly identified.

Further measurement areas showed typical background readings.

Intercomparison measurements between detector A, detector D and a prototype of a new measuring system (detector RLL) yielded comparable results if the raw data are evaluated with the software developed by Bucher (2001). There seems to be a weak indication of a lower detection efficiency of detector RLL.

Limits of the compensation of the count rate in different energy windows due to the presence of natural radionuclides (stripping correction) were found during the analysis of data over a Thorium anomaly using the method described in Schwarz (1991). Both over- and under-compensation was observed. This result indicates that the stripping correction cannot be separated completely into independent detector and flight specific parts and should be investigated further.

A source search exercise mainly targeted on the performance of first responders showed clearly that a deployment of airborne gamma spectrometry is not meaningful in cases where the location of sources is already known within the field of view of the detector.

A source search exercise in the framework of a large military exercise was effectively demonstrating the limits of the airborne gammaspectrometry system in respect to the location and identification of radionuclides. Sources of the radionuclides ^{137}Cs and ^{60}Co , which are identified automatically in the evaluation software, are located, identified and quantified effectually. The calculated activities of the sources agree well with the specified source activity. The uncertainties calculated according to Bucher, 2001 seem to be rather conservative and the respective algorithms should be inspected. No consistent over- or underestimation of activities was observed.

The detection of other radionuclides depends mainly on the skill and training of the operators. But even then, the performance of airborne gammaspectrometry has its limits. In the case of ^{241}Am , the spectral signal of a 1.8 GBq source does not suffice to render a signal observable in a search flight.

4 LITERATURE

Schwarz, G. F.: Methodische Entwicklungen zur Aerogammaspektrometrie. Beiträge zur Geologie der Schweiz, Geophysik Nr. 23, Schweizerische Geophysikalische Kommission, 1991.

Rybach, L., Schwarz, G. F. and Medici, F.: Construction of radioelement and dose-rate baseline maps by combining ground and airborne radiometric data. IAEA-Tecdoc-980, 33–44, Vienna, 1996

Schwarz, G.F., Rybach, L. and Klingel , E.: Design, calibration and application of an airborne gamma spectrometric system in Switzerland. Geophysics 62, 1369-1378, 1997

Bucher, B.: Methodische Weiterentwicklungen in der Aeroradiometrie. Dissertation Nr. 13973, ETH Z rich, 2001.

5 PREVIOUS REPORTS

Schwarz, G. F., Klingel , E. E., Rybach, L.: Aeroradiometrische Messungen in der Umgebung der schweizerischen Kernanlagen. Bericht f r das Jahr 1989 zuhanden der Hauptabteilung f r die Sicherheit der Kernanlagen (HSK). Interner Bericht, Institut f r Geophysik, ETH Z rich, 1990.

Schwarz, G. F., Klingel , E. E., Rybach, L.: Aeroradiometrische Messungen in der Umgebung der schweizerischen Kernanlagen. Bericht f r das Jahr 1990 zuhanden der Hauptabteilung f r die Sicherheit der Kernanlagen (HSK). Interner Bericht, Institut f r Geophysik, ETH Z rich, 1991.

Schwarz, G. F., Klingel , E. E., Rybach, L.: Aeroradiometrische Messungen in der Umgebung der schweizerischen Kernanlagen. Bericht f r das Jahr 1991 zuhanden der Hauptabteilung f r die Sicherheit der Kernanlagen (HSK). Interner Bericht, Institut f r Geophysik, ETH Z rich, 1992.

Schwarz, G. F., Klingel , E. E., Rybach, L.: Aeroradiometrische Messungen in der Umgebung der schweizerischen Kernanlagen. Bericht f r das Jahr 1992 zuhanden der Hauptabteilung f r die Sicherheit der Kernanlagen (HSK). Interner Bericht, Institut f r Geophysik, ETH Z rich, 1993.

Schwarz, G. F., Klingel , E. E., Rybach, L.: Aeroradiometrische Messungen in der Umgebung der schweizerischen Kernanlagen. Bericht f r das Jahr 1993 zuhanden der Hauptabteilung f r die Sicherheit der Kernanlagen (HSK). Interner Bericht, Institut f r Geophysik, ETH Z rich, 1994.

Schwarz, G. F., Rybach, L.: Aeroradiometrische Messungen im Rahmen der  bung ARM94. Bericht f r das Jahr 1994 zuhanden der Fachgruppe Aeroradiometrie (FAR). Interner Bericht, Institut f r Geophysik, ETH Z rich, 1995.

Schwarz, G. F., Rybach, L.: Aeroradiometrische Messungen im Rahmen der  bung ARM95. Bericht f r das Jahr 1995 zuhanden der Fachgruppe Aeroradiometrie (FAR). Interner Bericht, Institut f r Geophysik, ETH Z rich, 1996.

Schwarz, G. F., Rybach, L., B rlocher, C.: Aeroradiometrische Messungen im Rahmen der  bung ARM96. Bericht f r das Jahr 1996 zuhanden der Fachgruppe Aeroradiometrie (FAR). Interner Bericht, Institut f r Geophysik, ETH Z rich, 1997.

Bucher, B., Rybach, L., Schwarz, G., Bärlocher, C.: Aeroradiometrische Messungen im Rahmen der Übung ARM97. Bericht für das Jahr 1997 zuhanden der Fachgruppe Aeroradiometrie (FAR). Interner Bericht, Institut für Geophysik, ETH Zürich, 1998.

Bucher, B., Rybach, L., Schwarz, G., Bärlocher, C.: Aeroradiometrische Messungen im Rahmen der Übung ARM98. Bericht für das Jahr 1998 zuhanden der Fachgruppe Aeroradiometrie (FAR). Interner Bericht, Institut für Geophysik, ETH Zürich, 1999.

Bucher, B., Rybach, L., Schwarz, G., Bärlocher, C.: Aeroradiometrische Messungen im Rahmen der Übung ARM99. Bericht für das Jahr 1999 zuhanden der Fachgruppe Aeroradiometrie (FAR). Interner Bericht, Institut für Geophysik, ETH Zürich, 2000.

Bucher, B., Rybach, L., Schwarz, G., Bärlocher, C.: Aeroradiometrische Messungen im Rahmen der Übung ARM00. Bericht für das Jahr 2000 zuhanden der Fachgruppe Aeroradiometrie (FAR). Interner Bericht, Institut für Geophysik, ETH Zürich, 2001.

Bucher, B., Rybach, L., Schwarz, G., Bärlocher, C.: Aeroradiometrische Messungen im Rahmen der Übung ARM01. Bericht für das Jahr 2001 zuhanden der Fachgruppe Aeroradiometrie (FAR). Interner Bericht, Paul Scherrer Institut, Villigen, Schweiz, 2002.

Bucher, B., Rybach, L., Schwarz, G., Bärlocher, C.: Aeroradiometrische Messungen im Rahmen der Übung ARM02. Bericht für das Jahr 2002 zuhanden der Fachgruppe Aeroradiometrie (FAR). Interner Bericht, Paul Scherrer Institut, Villigen, Schweiz, 2003.

Bucher, B., Rybach, L., Schwarz, G.: Aeroradiometrische Messungen im Rahmen der Übung ARM03. PSI-Bericht 04-14, ISSN 1019-0643, Paul Scherrer Institut, Villigen, Schweiz, 2004.

Bucher, B., Butterweck, G., Rybach, L., Schwarz, G.: Aeroradiometrische Messungen im Rahmen der Übung ARM04. PSI-Bericht 05-10, ISSN 1019-0643, Paul Scherrer Institut, Villigen, Schweiz, 2005.

Bucher, B., Butterweck, G., Rybach, L., Schwarz, G.: Aeroradiometrische Messungen im Rahmen der Übung ARM05. PSI-Bericht 06-06, ISSN 1019-0643, Paul Scherrer Institut, Villigen, Schweiz, 2006.

Bucher, B., Butterweck, G., Rybach, L., Schwarz, G.: Aeroradiometrische Messungen im Rahmen der Übung ARM06. PSI-Bericht 07-02, ISSN 1019-0643, Paul Scherrer Institut, Villigen, Schweiz, 2007.

Bucher, B., Guillot, L., Strobl, C., Butterweck, G., Gutierrez, S., Thomas, M., Hohmann, C., Krol, I., Rybach, L., Schwarz, G.: International Intercomparison Exercise of Airborne Gammaspectrometric Systems of Germany, France and Switzerland in the Framework of the Swiss Exercise ARM07. PSI-Bericht Nr. 09-07, ISSN 1019-0643, Paul Scherrer Institut, Villigen, Schweiz, 2009.

Bucher, B., Butterweck, G., Rybach, L., Schwarz, G.: Aeroradiometrische Messungen im Rahmen der Übung ARM08. PSI-Bericht Nr. 09-02, ISSN 1019-0643, Paul Scherrer Institut, Villigen, Schweiz, 2009.

Bucher, B., Butterweck, G., Rybach, L., Schwarz, G., Strobl, C.: Aeroradiometrische Messungen im Rahmen der Übung ARM09. PSI-Bericht Nr. 10-01, ISSN 1019-0643, Paul Scherrer Institut, Villigen, Schweiz, 2010.

Bucher, B., Butterweck, G., Rybach, L., Schwarz, G., Mayer, S.: Aeroradiometrische Messungen im Rahmen der Übung ARM10. PSI-Bericht Nr. 11-02, ISSN 1019-0643, Paul Scherrer Institut, Villigen, Schweiz, 2011.

Bucher, B., Butterweck, G., Rybach, L., Schwarz, G., Mayer, S.: Aeroradiometric Measurements in the Framework of the Swiss Exercise ARM11. PSI-Report No. 12-04, ISSN 1019-0643, Paul Scherrer Institut, Villigen, Switzerland, 2012.

Butterweck, G., Bucher, B., Rybach, L., Schwarz, G., Hödlmoser, H., Mayer, S., Danzi, C. Scharding, G.: Aeroradiometric Measurements in the Framework of the Swiss Exercise ARM12. PSI-Report No. 13-01, ISSN 1019-0643, Paul Scherrer Institut, Villigen, Switzerland, 2013.

Butterweck, G., Bucher, B., Rybach, L., Schwarz, G., Hohmann, E., Mayer, S., Danzi, C. Scharding, G.: Aeroradiometric Measurements in the Framework of the Swiss Exercise ARM13. PSI-Report No. 15-01, ISSN 1019-0643, Paul Scherrer Institut, Villigen, Switzerland, 2015.

The reports since 1994 can be found and downloaded from the FAR website <http://www.far.ensi.ch>.

6 EVALUATION PARAMETER FILES

The parameter files used for the evaluation of raw data in this report are listed below to improve the traceability of the presented results. The detector definition files have been re-evaluated for all detectors. Therefore, the definition file of detector C, which was not used in this year are also listed.

6.1 DefinitionFile_Processing.txt

This file defines the parameters used for the gridding of evaluated parameters.

----- Start of file -----

Definition file Swiss MGS32

"Windows"

10

Total 401. 2997. 0. 0

K-40 1369. 1558. 1460. 1

U-238 1664. 1853. 1765. 1

Th-232 2407. 2797. 2615. 1

Cs-137 600. 720. 660. 2

Co-60 1100. 1400. 0. 2

MMGC1 400. 1400. 0. 0

MMGC2 1400. 2997. 0. 0

LOW 40. 720. 0. 0

MID 720. 2997. 0. 0

"Ratios"

3

MMGCVerhältnis MMGC1 MMGC2 Ratio_MMGC

LOWHigh LOW MMGC2 RatioLowHigh

LowMid LOW MID RatioLowMid

"Conversion factors Activity to Dose Rate"

8

Total 0 NoCalibration " " 0

AD_K-40 0.044 DHSR "nSv/h" 1

AD_U-238 0.55 DHSR "nSv/h" 1

AD_Th-232 0.77 DHSR "nSv/h" 1

AD_Cs-137 0.2 DHSR "nSv/h" 2

Co-60 0 NoCalibration " " 0

MMGC1 0 NoCalibration " " 0

MMGC2 0 NoCalibration " " 0

"Typ des Darstellungsgrenzwertes"

1

Nachweistyp 0

"counts of spectra to stack"

1

Counts 1

"Auszugebende Werte"

30

"DHSR TOT ", "DHSR_TOT", "nSv/h ", 0.00, 250.00

"AP_Co-60 ", "AP_Co-60", "MBq ", 0.00, 150.00

"AP_Cs-137 ", "AP_Cs-137", "MBq ", 0.00, 40.00

"Terr. DL ", "DHSR_TOT", "nSv/h ", 0.00, 250.00

"CR_Caesium ", "CR_Cs-137", "cps ", 20.00, 120.00

"CR_Cobalt ", "CR_Co-60", "cps ", 0.00, 100.00

"NR_Caesium ", "NR_Cs-137", "cps ", 0.00, 120.00

"NR_Cobalt ", "NR_Co-60", "cps ", 0.00, 100.00

"Total_CR_corr ", "NR_Total", "cps ", 200.00, 1200.00

"K-40 ", "AD_K-40", "Bq/kg ", 0.00, 1000.00

"U-238 ", "AD_U-238", "Bq/kg ", 0.00, 120.00

"Th-232 ", "AD_Th-232", "Bq/kg ", 0.00, 120.00

"Cs-137 ", "AD_Cs-137", "Bq/kg ", 0.00, 240.00

"Cobalt_CR ", "NR_Co-60", "cps ", 0.00, 120.00

```

"Nat.Terr.DL      ", "DHSR_NAT", "nSv/h  ", 0.00, 250.00
"Künst.DL        ", "DHSR_ANT", "nSv/h  ", 0.00, 250.00
"MMGC_Ratio      ", "MMGC_Ratio", "%      ", 400, 600.00
"Cosmic DL        ", "DHSR_COS", "nSv/h  ", 20.00, 60.00
"Cosmic           ", "CR_COS", "cps    ", 000.00, 400.00
"Radar           ", "PH", "m      ", 0.00, 300.00
"ODL             ", "DHSR", "nSv/h  ", 0.00, 250
"AD_UT_K-40      ", "AD_UT_K-40", "Bq/kg   ", 0.00, 200
"AD_UT_U-238     ", "AD_UT_U-238", "Bq/kg   ", 0.00, 50
"AD_UT_Th-232    ", "AD_UT_Th-232", "Bq/kg   ", 0.00, 40
"AD_UT-Cs-137    ", "AD_UT-Cs-137", "Bq/kg   ", 0.00, 20
"Err_Co-60       ", "NR_UT_Co-60", "cps     ", 0.00, 40
"Nachweis_Cs-137 ", "CR_LD_Cs-137", "cps     ", 0.00, 100.00
"Nachweis_Co-60  ", "CR_LD_Co-60", "cps     ", 0.00, 100.00
"Cs-137 beta=0   ", "AA_Cs-137", "Bq/m2   ", 0.00, 20000.00
"AA_UT-Cs-137    ", "AA_UT-Cs-137", "Bq/m2   ", 0.00, 20
----- End of file -----

```

6.2 Processing_Quellensuche.txt

This file defines the parameters used for the gridding of evaluated parameters for the special case of a source search.

----- Start of file -----

Definition file Swiss MGS32

"Windows"

10

```

Total  401.  2997.  0.  0
K-40   1369.  1558.  1460.  1
U-238  1664.  1853.  1765.  1
Th-232 2407.  2797.  2615.  1
Cs-137  600.  720.  660.  2
Co-60  1100.  1400.  0.  2
MMGC1   400.  1400.  0.  0
MMGC2  1400.  2997.  0.  0
LOW     40.  720.  0.  0
MID    720.  2997.  0.  0

```

"Ratios"

3

MMGCVerhältnis MMGC1 MMGC2 Ratio_MMGC

LOWHigh LOW MMGC2 RatioLowHigh

LowMid LOW MID RatioLowMid

"Conversion factors Activity to Dose Rate"

8

Total 0 NoCalibration " " 0

AD_K-40 0.044 DHSR "nSv/h" 1

AD_U-238 0.55 DHSR "nSv/h" 1

AD_Th-232 0.77 DHSR "nSv/h" 1

AD_Cs-137 0.2 DHSR "nSv/h" 2

Co-60 0 NoCalibration " " 0

MMGC1 0 NoCalibration " " 0

MMGC2 0 NoCalibration " " 0

"Typ des Darstellungsgrenzwertes"

1

Nachweistyp 0

"counts of spectra to stack"

1

Counts 1

"Auszugebende Werte"

30

"DHSR TOT ", "DHSR_TOT", "nSv/h ", 0.00, 250.00

"AP_Co-60 ", "AP_Co-60", "MBq ", 0.00, 150.00

"AP_Cs-137 ", "AP_Cs-137", "MBq ", 0.00, 40.00

"Terr. DL ", "DHSR_TOT", "nSv/h ", 0.00, 250.00

"CR_Caesium ", "CR_Cs-137", "cps ", 20.00, 120.00

"CR_Cobalt ", "CR_Co-60", "cps ", 0.00, 100.00

"NR_Caesium ", "NR_Cs-137", "cps ", 0.00, 120.00

"NR_Cobalt ", "NR_Co-60", "cps ", 0.00, 100.00

"AP_UT_Cs-137 ", "AP_UT_Cs-137", "MBq ", 0.00, 5000.00

"K-40 ", "AD_K-40", "Bq/kg ", 0.00, 1000.00

"U-238 ", "AD_U-238", "Bq/kg ", 0.00, 120.00

"Th-232 ", "AD_Th-232", "Bq/kg ", 0.00, 120.00

"Cs-137 ", "AD_Cs-137", "Bq/kg ", 0.00, 240.00

"Cobalt_CR ", "NR_Co-60", "cps ", 0.00, 120.00


```

"Nat.Terr.DL      ", "DHSR_NAT", "nSv/h  ", 0.00, 250.00
"Künst.DL        ", "DHSR_ANT", "nSv/h  ", 0.00, 250.00
"MMGC_Ratio      ", "MMGC_Ratio", "%      ", 400, 600.00
"Cosmic DL        ", "DHSR_COS", "nSv/h  ", 20.00, 60.00
"Cosmic           ", "CR_COS", "cps    ", 000.00, 400.00
"Radar           ", "PH", "m      ", 0.00, 300.00
"ODL             ", "DHSR", "nSv/h  ", 0.00, 250
"AD_UT_K-40      ", "AD_UT_K-40", "Bq/kg   ", 0.00, 200
"AD_UT_U-238     ", "AD_UT_U-238", "Bq/kg   ", 0.00, 50
"AD_UT_Th-232    ", "AD_UT_Th-232", "Bq/kg   ", 0.00, 40
"AD_UT_Cs-137    ", "AD_UT_Cs-137", "Bq/kg   ", 0.00, 20
"AP_UT_Co-60     ", "AP_UT_Co-60", "MBq     ", 0.00, 1000
"Nachweis_Cs-137 ", "CR_LD_Cs-137", "cps     ", 0.00, 100.00
"Nachweis_Co-60  ", "CR_LD_Co-60", "cps     ", 0.00, 100.00
"Cs-137 beta=0   ", "AA_Cs-137", "Bq/m2   ", 0.00, 20000.00
"AA_UT_Cs-137    ", "AA_UT_Cs-137", "Bq/m2   ", 0.00, 20
----- End of file -----

```

6.3 DefinitionFile_DetA.txt

This file defines the parameters used for the derivation of dose rates and activity concentrations from the raw spectra. Detector A is a 16-litre-detector produced by Exploranium more than 25 years ago. This detector is used only as backup to detectors C and D.

```

----- Start of file -----
Definition file System
"Koordinaten"
WGS84
"Non-linearity"
4
a0 3.63525
a1 0.0829776
a2 -0.000000771333
a3 0
"Recorder old RDT-Files"
8
Radar 0.00 -61.00
Baro 0.74 457.14
Cosm 0.00 1.00
Dead 5.00 0.00
Time 0.00 1.00
Temp 0.00 1.00

```

Pitch 0.00 76.20

Roll 0.00 90.91

"Background/Cosmic"

10

Total	98.1000	1.041	0.032
K-40	12.100	0.050	0.004
U-238	2.700	0.043	0.002
Th-232	3.400	0.044	0.001
Cs-137	15.500	0.102	0.005
Co-60	13.900	0.100	0.004
MMGC1	79.540	0.771	0.019
MMGC2	18.500	0.270	0.007
LOW	0.	0.	0.
MID	0.	0.	0.

"Stripping Coefficients"

10

1.000	0.000	0.000	0.000	0.000	0.000	0.000	0.000	0.000	0.000
0.000	1.000	0.971	0.472	0.000	0.048	0.000	0.000	0.000	0.000
0.000	-0.001	1.000	0.315	0.000	-0.007	0.000	0.000	0.000	0.000
0.000	-0.002	0.069	1.000	0.000	-0.003	0.000	0.000	0.000	0.000
0.000	0.397	3.541	1.706	1.000	0.089	0.000	0.000	0.000	0.000
0.000	0.707	2.453	0.748	0.000	1.000	0.000	0.000	0.000	0.000
0.000	0.000	0.000	0.000	0.000	0.000	1.000	0.000	0.000	0.000
0.000	0.000	0.000	0.000	0.000	0.000	0.000	1.000	0.000	0.000
0.000	0.000	0.000	0.000	0.000	0.000	0.000	0.000	1.000	0.000
0.000	0.000	0.000	0.000	0.000	0.000	0.000	0.000	0.000	1.000

"Converted Stripping Coefficients Matrix"

10

1.000	0.000	0.000	0.000	0.000	0.000	0.000	0.000	0.000	0.000
0.000	1.038	-0.858	-0.177	0.000	-0.056	0.000	0.000	0.000	0.000
0.000	-0.004	1.010	-0.321	0.000	0.006	0.000	0.000	0.000	0.000
0.000	0.000	-0.077	1.022	0.000	0.003	0.000	0.000	0.000	0.000
0.000	-0.335	-2.943	-0.548	1.000	-0.096	0.000	0.000	0.000	0.000
0.000	-0.725	-1.813	0.149	0.000	1.022	0.000	0.000	0.000	0.000
0.000	0.000	0.000	0.000	0.000	0.000	1.000	0.000	0.000	0.000
0.000	0.000	0.000	0.000	0.000	0.000	0.000	1.000	0.000	0.000
0.000	0.000	0.000	0.000	0.000	0.000	0.000	0.000	1.000	0.000
0.000	0.000	0.000	0.000	0.000	0.000	0.000	0.000	0.000	1.000

"Sigma of Converted Stripping Coefficients Matrix"

10

0.000	0.000	0.000	0.000	0.000	0.000	0.000	0.000	0.000	0.000
0.000	0.000	-0.040	-0.017	0.000	-0.016	0.000	0.000	0.000	0.000
0.000	0.000	0.000	-0.028	0.000	0.000	0.000	0.000	0.000	0.000
0.000	0.000	-0.009	0.000	0.000	0.000	0.000	0.000	0.000	0.000
0.000	-0.080	-0.103	-0.037	0.000	-0.008	0.000	0.000	0.000	0.000
0.000	-0.140	-0.068	0.013	0.000	0.000	0.000	0.000	0.000	0.000
0.000	0.000	0.000	0.000	0.000	0.000	0.000	0.000	0.000	0.000
0.000	0.000	0.000	0.000	0.000	0.000	0.000	0.000	0.000	0.000
0.000	0.000	0.000	0.000	0.000	0.000	0.000	0.000	0.000	0.000
0.000	0.000	0.000	0.000	0.000	0.000	0.000	0.000	0.000	0.000

"Attenuation Coefficients"

10

Total	0.00600	1.00000	0.0003
K-40	0.00800	1.00000	0.0008
U-238	0.00550	1.00000	0.0114
Th-232	0.00600	1.00000	0.0044
Cs-137	0.01000	1.00000	0.0100
Co-60	0.00800	1.00000	0.0080
MMGC1	0.00600	1.00000	0.0060
MMGC2	0.00650	1.00000	0.0065
LOW	0.02000	1.00000	0.01
MID	0.01500	1.00000	0.005

"3D Attenuation Coefficients"

10

Total	0.00350	2.00000
K-40	0.00420	2.00000
U-238	0.00320	2.00000
Th-232	0.00350	2.00000
Cs-137	0.00800	2.00000
Co-60	0.00800	1.00000
MMGC1	0.00600	1.00000
MMGC2	0.00650	1.00000
LOW	0.02000	1.00000
MID	0.01500	1.00000

"Conversion factors Counts to Activity"

11

Total	0	NoCalibration	" "
K-40	8.29	AD_K-40	"Bq/kg"
U-238	4.0	AD_U-238	"Bq/kg"
Th-232	1.67	AD_Th-232	"Bq/kg"
Cs-137	2.0	AD_Cs-137	"Bq/kg"
Cs-137	35.0	AA_Cs-137	"Bq/m2"
Cs-137	7.2	AP_Cs-137	"MBq "
Co-60	2.5	AP_Co-60	"MBq "
Co-60	0	NoCalibration	" "
MMGC1	0	NoCalibration	" "
MMGC2	0	NoCalibration	" "

"Radon"

1

0 0

"Hoehenkorrektur"

3

1

1

PfadDHM25 C:\DATEN\Benno\Aeroradiometrie\Daten\DHM25\

"SDI Constants"

7

Aten	0.0056
Convert	0.00096
CosmicKorr	95.5
Back	12640.0
Gain	12.0


```

referenz_alt 100.0
Threshold 240.0
----- End of file -----

```

6.4 DefinitionFile_DetC.txt

This file defines the parameters used for the derivation of dose rates and activity concentrations from the raw spectra. The current file is customized for the 16-litre-detector purchased from Exploranium in the year 2007. This detector was used for most measurements since the year 2007 but was not available in the exercise ARM14 for logistical reasons.

```

----- Start of file -----
Definition file System
"Koordinaten"
WGS84
"Non-linearity"
4
a0 0.6966
a1 0.08423
a2 -0.0000032807
a3 0.0000000042937
"Recorder old RDT-Files"
8
Radar 0.00 -61.00
Baro 0.74 457.14
Cosm 0.00 1.00
Dead 5.00 0.00
Time 0.00 1.00
Temp 0.00 1.00
Pitch 0.00 76.20
Roll 0.00 90.91
"Background/Cosmic"
10
Total 98.1000 1.041 0.032
K-40 12.100 0.050 0.004
U-238 2.700 0.043 0.002
Th-232 3.400 0.044 0.001
Cs-137 15.500 0.102 0.005
Co-60 13.900 0.100 0.004
MMGC1 79.540 0.771 0.019
MMGC2 18.500 0.270 0.007
LOW 0. 0. 0.
MID 0. 0. 0.
"Stripping Coefficients"
10
1.000 0.000 0.000 0.000 0.000 0.000 0.000 0.000 0.000 0.000
0.000 1.000 0.710 0.350 0.000 0.070 0.000 0.000 0.000 0.000
0.000 -0.020 1.000 0.210 0.000 -0.010 0.000 0.000 0.000 0.000
0.000 -0.010 0.040 1.000 0.000 0.000 0.000 0.000 0.000 0.000

```

0.000	0.060	3.760	2.340	1.000	0.170	0.000	0.000	0.000	0.000
0.000	0.280	2.360	0.550	0.000	1.000	0.000	0.000	0.000	0.000
0.000	0.000	0.000	0.000	0.000	0.000	1.000	0.000	0.000	0.000
0.000	0.000	0.000	0.000	0.000	0.000	0.000	1.000	0.000	0.000
0.000	0.000	0.000	0.000	0.000	0.000	0.000	0.000	1.000	0.000
0.000	0.000	0.000	0.000	0.000	0.000	0.000	0.000	0.000	1.000

"Converted Stripping Coefficients Matrix"

10

1.000	0.000	0.000	0.000	0.000	0.000	0.000	0.000	0.000	0.000
0.000	1.030	-0.730	-0.200	0.000	-0.070	0.000	0.000	0.000	0.000
0.000	0.020	0.980	-0.340	0.000	0.010	0.000	0.000	0.000	0.000
0.000	0.010	-0.050	1.010	0.000	0.000	0.000	0.000	0.000	0.000
0.000	-0.280	-3.230	-1.180	1.000	-0.170	0.000	0.000	0.000	0.000
0.000	-0.700	-2.120	0.260	0.000	1.030	0.000	0.000	0.000	0.000
0.000	0.000	0.000	0.000	0.000	0.000	1.000	0.000	0.000	0.000
0.000	0.000	0.000	0.000	0.000	0.000	0.000	1.000	0.000	0.000
0.000	0.000	0.000	0.000	0.000	0.000	0.000	0.000	1.000	0.000
0.000	0.000	0.000	0.000	0.000	0.000	0.000	0.000	0.000	1.000

"Sigma of Converted Stripping Coefficients Matrix"

10

0.000	0.000	0.000	0.000	0.000	0.000	0.000	0.000	0.000	0.000
0.000	0.000	-0.040	-0.017	0.000	-0.016	0.000	0.000	0.000	0.000
0.000	0.000	0.000	-0.028	0.000	0.000	0.000	0.000	0.000	0.000
0.000	0.000	-0.009	0.000	0.000	0.000	0.000	0.000	0.000	0.000
0.000	-0.080	-0.103	-0.037	0.000	-0.008	0.000	0.000	0.000	0.000
0.000	-0.140	-0.068	0.013	0.000	0.000	0.000	0.000	0.000	0.000
0.000	0.000	0.000	0.000	0.000	0.000	0.000	0.000	0.000	0.000
0.000	0.000	0.000	0.000	0.000	0.000	0.000	0.000	0.000	0.000
0.000	0.000	0.000	0.000	0.000	0.000	0.000	0.000	0.000	0.000
0.000	0.000	0.000	0.000	0.000	0.000	0.000	0.000	0.000	0.000

"Attenuation Coefficients"

10

Total	0.00600	1.00000	0.0003
K-40	0.00800	1.00000	0.0008
U-238	0.00550	1.00000	0.0114
Th-232	0.00600	1.00000	0.0044
Cs-137	0.01000	1.00000	0.0100
Co-60	0.00800	1.00000	0.0080
MMGC1	0.00600	1.00000	0.0060
MMGC2	0.00650	1.00000	0.0065
LOW	0.02000	1.00000	0.01
MID	0.01500	1.00000	0.005

"3D Attenuation Coefficients"

10

Total	0.00350	2.00000
K-40	0.00420	2.00000
U-238	0.00320	2.00000
Th-232	0.00350	2.00000
Cs-137	0.00800	2.00000
Co-60	0.00800	1.00000
MMGC1	0.00600	1.00000

```

MMGC2    0.00650  1.00000
LOW      0.02000  1.00000
MID      0.01500  1.00000
"Conversion factors Counts to Activity"
11
Total    0      NoCalibration  "  "
K-40     7.95   AD_K-40      "Bq/kg"
U-238    3.87   AD_U-238     "Bq/kg"
Th-232   1.62   AD_Th-232   "Bq/kg"
Cs-137   1.88   AD_Cs-137   "Bq/kg"
Cs-137   32.96  AA_Cs-137   "Bq/m2"
Cs-137   7.2    AP_Cs-137   "MBq "
Co-60    2.5    AP_Co-60    "MBq "
Co-60    0      NoCalibration  "  "
MMGC1    0      NoCalibration  "  "
MMGC2    0      NoCalibration  "  "
"Radon"
1
0      0
"Hoehenkorrektur"
3
1
1
PfadDHM25 K:\Aeroradiometrie\GammaMap\DHM25\
"SDI Constants"
7
Aten     0.0053
Convert  0.00096
CosmicKorr 95.5
Back     12640.0
Gain     12.0
referenz_alt 100.0
Threshold 240.0
----- End of file -----

```

6.5 DefinitionFile_DetD.txt

This file defines the parameters used for the derivation of dose rates and activity concentrations from the raw spectra. The current file is customized for a 16-litre-detector with integrated multichannel analyser purchased from Radiation Solutions in the year 2013. This detector was used in the exercise ARM14 for the first time.

```

----- Start of file -----
Definition file System
"Koordinaten"
WGS84
"Non-linearity"
4
a0 1.8745
a1 0.082009

```


0.000	0.000	-0.040	-0.017	0.000	-0.016	0.000	0.000	0.000	0.000
0.000	0.000	0.000	-0.028	0.000	0.000	0.000	0.000	0.000	0.000
0.000	0.000	-0.009	0.000	0.000	0.000	0.000	0.000	0.000	0.000
0.000	-0.080	-0.103	-0.037	0.000	-0.008	0.000	0.000	0.000	0.000
0.000	-0.140	-0.068	0.013	0.000	0.000	0.000	0.000	0.000	0.000
0.000	0.000	0.000	0.000	0.000	0.000	0.000	0.000	0.000	0.000
0.000	0.000	0.000	0.000	0.000	0.000	0.000	0.000	0.000	0.000
0.000	0.000	0.000	0.000	0.000	0.000	0.000	0.000	0.000	0.000
0.000	0.000	0.000	0.000	0.000	0.000	0.000	0.000	0.000	0.000
0.000	0.000	0.000	0.000	0.000	0.000	0.000	0.000	0.000	0.000

"Attenuation Coefficients"

10

Total	0.00600	1.00000	0.0003
K-40	0.00800	1.00000	0.0008
U-238	0.00550	1.00000	0.0114
Th-232	0.00600	1.00000	0.0044
Cs-137	0.01000	1.00000	0.0100
Co-60	0.00800	1.00000	0.0080
MMGC1	0.00600	1.00000	0.0060
MMGC2	0.00650	1.00000	0.0065
LOW	0.02000	1.00000	0.01
MID	0.01500	1.00000	0.005

"3D Attenuation Coefficients"

10

Total	0.00350	2.00000
K-40	0.00420	2.00000
U-238	0.00320	2.00000
Th-232	0.00350	2.00000
Cs-137	0.00800	2.00000
Co-60	0.00800	1.00000
MMGC1	0.00600	1.00000
MMGC2	0.00650	1.00000
LOW	0.02000	1.00000
MID	0.01500	1.00000

"Conversion factors Counts to Activity"

11

Total	0	NoCalibration	" "
K-40	7.95	AD_K-40	"Bq/kg"
U-238	3.87	AD_U-238	"Bq/kg"
Th-232	1.62	AD_Th-232	"Bq/kg"
Cs-137	1.88	AD_Cs-137	"Bq/kg"
Cs-137	32.96	AA_Cs-137	"Bq/m2"
Cs-137	7.2	AP_Cs-137	"MBq "
Co-60	2.5	AP_Co-60	"MBq "
Co-60	0	NoCalibration	" "
MMGC1	0	NoCalibration	" "
MMGC2	0	NoCalibration	" "

"Radon"

1

0 0

"Hoehenkorrektur"

3

1

1

PfadDHM25 C:\DATEN\Benno\Aeroradiometrie\Daten\DHM25\
"SDI Constants"

7

Aten 0.0053

Convert 0.00096

CosmicKorr 95.5

Back 12640.0

Gain 12.0

referenz_alt 100.0

Threshold 240.0

----- End of file -----

Paul Scherrer Institut :: 5232 Villigen PSI :: Switzerland :: Tel. +41 56 310 21 11 :: Fax +41 56 310 21 99 :: www.psi.ch

